AD A086 992   GTE LABS INC WALTHAM MA   F/G 10/3
INVESTIGATION OF METHODS TO ELIMINATE VOLTAGE DELAY IN LI/SOCL2--ETC(U)
MAY 80   C SCHLAIKJER, C A YOUNG, M DOBRUSIN   DAAB07-78-C-0558
UNCLASSIFIED   DELET-TR-78-0558-1F   NL

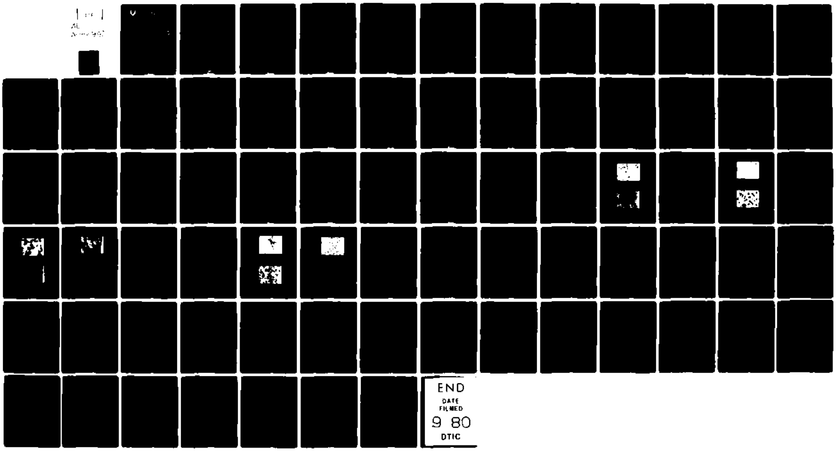

END
DATE
FILMED
9 80
DTIC

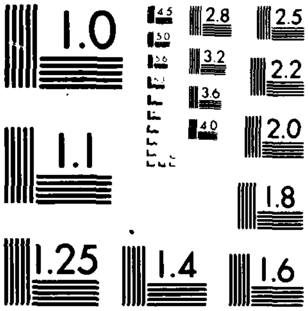
1.0
4.5
5.0
5.6
2.8
3.2
3.6
4.0
2.5
2.2
2.0
1.1
1.8
1.25
1.4
1.6

LEVEL II

Ⓡ

Research and Development Technical Report

DELET–TR–78–0558.1F

ADA086992

INVESTIGATION OF METHODS TO ELIMINATE VOLTAGE DELAY IN Li/$SOCl_2$ CELLS

DTIC
ELECTE
JUL 22 1980
S D
C

C. Schlaikjer
C.A. Young
M. Dobrusin

GTE LABORATORIES INCORPORATED
40 Sylvan Road
Waltham, Massachusetts 02154

May 1980

Final Report for Period 19 September 1978 – 19 September 1979

DISTRIBUTION STATEMENT

Approved for public release;
distribution unlimited.

Prepared for:

ELECTRONICS TECHNOLOGY & DEVICES LABORATORY

ERADCOM

US ARMY ELECTRONICS RESEARCH AND DEVELOPMENT COMMAND
FORT MONMOUTH, NEW JERSEY 07703

DDC FILE COPY

80 7 18 042

HISA–FM 196–7

NOTICES

Disclaimers

Disposition

HISA–FM–633–78

UNCLASSIFIED

SECURITY CLASSIFICATION OF THIS PAGE (*When Data Entered*)

REPORT DOCUMENTATION PAGE

READ INSTRUCTIONS
BEFORE COMPLETING FORM

1. REPORT NUMBER (18) DELET/TR-78-0558-F	2. GOVT ACCESSION NO. AD-A086992	3. RECIPIENT'S CATALOG NUMBER
4. TITLE (and Subtitle) (6) INVESTIGATION OF METHODS TO ELIMINATE VOLTAGE DELAY IN Li/$SOCl_2$ CELLS.		5. TYPE OF REPORT & PERIOD COVERED (9) FINAL REPORT. 19 Sep 78 — 19 Sep 79
		6. PERFORMING ORG. REPORT NUMBER 78-0558-F
7. AUTHOR(s) (10) Carl/Schlaikjer Clifton A./Young Marc/Dobrusin		8. CONTRACT OR GRANT NUMBER(s) (15) DAAB07-78-C-0558
9. PERFORMING ORGANIZATION NAME AND ADDRESS GTE Laboratories Incorporated 40 Sylvan Road Waltham, Mass 02154		10. PROGRAM ELEMENT, PROJECT, TASK AREA & WORK UNIT NUMBERS (16) 1L161102 AH47-03-483
11. CONTROLLING OFFICE NAME AND ADDRESS US Army Electronics Technology & Devices Lab (ERADCOM), ATTN: DELET-PR Fort Monmouth, NJ 07703		12. REPORT DATE (11) May 1980 (17) 03
		13. NUMBER OF PAGES 87
14. MONITORING AGENCY NAME & ADDRESS(*if different from Controlling Office*) (12) 75		15. SECURITY CLASS. (*of this report*) UNCLASSIFIED
		15a. DECLASSIFICATION/DOWNGRADING SCHEDULE

16. DISTRIBUTION STATEMENT (*of this Report*)

Approved for Public Release; distribution unlimited.

17. DISTRIBUTION STATEMENT (*of the abstract entered in Block 20, if different from Report*)

(19) TR-78-0558-1F

18. SUPPLEMENTARY NOTES

19. KEY WORDS (*Continue on reverse side if necessary and identify by block number*)

Lithium-thionyl chloride cells, voltage delay, lithium passivation, inorganic electrolyte batteries, polyhedral borate, nonaqueous batteries.

20. ABSTRACT (*Continue on reverse side if necessary and identify by block number*)

A comparative study of thionyl chloride electrolytes containing $LiAlCl_4^-$, $Li_2^+B_{10}Cl_{10}^=$, or $Li_2^+B_{12}Cl_{12}^=$ has been carried out by monitoring LiCl film growth on lithium samples stored in these electrolytes and by evaluating the startup and measuring the capacity of anode limited lithium/thionyl chloride cells. The film growth on lithium samples was monitored by galvanostatic pulse polarization, by weight gain analysis, and by examination under the scanning electron microscope. The film →

DD FORM 1 JAN 73 1473 EDITION OF 1 NOV 65 IS OBSOLETE

UNCLASSIFIED

SECURITY CLASSIFICATION OF THIS PAGE (*When Data Entered*)

406462 Gu

Item 20 - Abstract (Continued)

growth rate on lithium in $Li_2B_{10}Cl_{10}/SOCl_2$ was found to be comparable to that in pure $SOCl_2$, about one tenth of that found in $LiAlCl_4/SOCl_2$. Storage for longer periods of time or higher temperatures caused thicker films to form. The polyhedral borate electrolyte produced smooth films on lithium with widely scattered crystals, instead of closely packed crystals as in $LiAlCl_4/SOCl_2$. Lithium/thionyl chloride cells containing $Li_2B_{10}Cl_{10}/SOCl_2$ started without delay at -20°C, even after prolonged storage at elevated temperature. The polyhedral borate electrolyte also reduced self discharge by local cell reduction of the solvent against cell hardware connected to the anode. The specific conductivity of $Li_2B_{10}Cl_{10}/SOCl_2$, $Li_2B_{12}Cl_{12}/SOCl_2$, and $LiAlCl_4/SOCl_2$ were compared as a function of concentration and temperature, and the visible and EPR spectra of $Li_2B_{10}Cl_{10}/SOCl_2$ taken. A stable free radical with an unusually wide peak width was found.

FOREWORD

Some of the results described in this report were not obtained specifically for this contract, but have been included because of their relevance to the particular subject.

TABLE OF CONTENTS

TABLE OF CONTENTS (Continued)

LIST OF ILLUSTRATIONS

LIST OF ILLUSTRATIONS (Continued)

LIST OF ILLUSTRATIONS (Continued)

LIST OF TABLES

1. INTRODUCTION

The object of this work has been to prepare a fundamental study of the formation and growth of lithium chloride films on lithium metal exposed to thionyl chloride electrolytes, and to determine how the electrolyte salts, $LiAlCl_4$, $Li_2B_{10}Cl_{10}$ and $Li_2B_{12}Cl_{12}$, affect both the film growth and the voltage delay or startup characteristic of primary cells following storage at ambient or elevated temperature. The thickness of the lithium chloride film on lithium in these cells has been correlated with the severity of the voltage delay following storage (1-5). The salt $Li_2B_{10}Cl_{10}$ was reported to alleviate voltage delay when used in place of $LiAlCl_4$, although the mechanism responsible for this dramatic improvement was not established (20).

We intended to determine to what extent the polyhedral borate salts are more effective than lithium tetrachloroaluminate in preventing heavy film formation, electrochemical passivation, and voltage delay, and to establish by what mechanisms the polyhedral borate salts are able to accomplish their effect. An adequate solution to the delay problem would require that neither anode corrosion, self-discharge, or other cell deterioration is a consequence of any changes made in the electrolyte composition. If the borate salts should prove to be substantially more effective than $LiAlCl_4$ as electrolytes in $Li/SOCl_2$ power sources, an understanding of the mechanism by which this occurs could make alternative solutions possible.

The thickness and resistivity of films on active metals in corrosive electrolytes have been measured using a galvanostatic pulse technique and by the weight gain of lithium samples stored with electrolytes in glass ampoules (6-10). These studies have led to the development of the solid electrolyte interphase (SEI) model for these systems. According to this theory, contact between lithium and solutions containing thionyl chloride causes the formation of a thin insoluble film of lithium chloride which completely covers the metal, preventing further rapid chemical attack by stopping solvent transport, but allowing anodic discharge by permitting the passage of lithium ions. The theory proposes that the film consists of two layers. The first, a thin compact layer next to the metal and referred to as the SEI, is said to be overlain with a porous and much thicker layer of lithium chloride crystals. The outer layer is thought to be responsible for the voltage delay (10).

Investigations over the past several years have demonstrated that significant improvements in the voltage delay characteristic and in reducing the corrosion of lithium anodes are possible using lithium tetrachloroaluminate as the electrolyte salt (3,5,38). Iron and copper have been reported to aggravate the growth of the lithium chloride film, and HCl and

$AlCl_3OH^-$, products of electrolyte hydrolysis (39), also contribute to excessive anode film growth and corrosion. The practical limit to the improvement of cells containing $LiAlCl_4$ by removal of these impurities has not been determined. If there is a limit, it should be established to provide a basis on which to claim further improvement simultaneously in reduction of the voltage delay and of anode corrosion. For this reason we have chosen to include $LiAlCl_4$ electrolytes in our investigations.

These investigations encompass galvanostatic measurements of film thickness and resistivity, corrosion measurements by weight gain of lithium samples stored with electrolytes, and voltage delay and capacity measurements on complete cells as a function of storage temperature and time. The galvanostatic measurements were planned to be carried out essentially by the methods developed previously (6-10). As a comparison to the weight gain measurements, lithium samples were to be compared in the scanning electron microscope to observe the morphology of the surface layers. The complete cells were to be anode limited in order to measure capacity losses during storage as well as passivation and voltage delay.

2. EXPERIMENTAL

2.1 PURIFICATION OF THIONYL CHLORIDE

Thionyl chloride, obtained from Mobay or Hooker Chemical, contains minor amounts of SO_2Cl_2, S_2Cl_2, SCl_2, and sometimes sulfur. Distillation from triphenylphosphite (11) removes these impurities by reducing them to phosphate, thiophosphate, and chlorophosphate esters with low-vapor pressures. Fractionation of the mixture affords a distillate with reduced amounts of these materials. SO_2 and HCl are not removed, but refluxing over lithium and fractionation was found to remove HCl (12). The solvent used was water white, and the HCl content was below the limit of detection using a quartz windowed 1 cm pathlength cell at 2775 cm^{-1} on a Beckman IR-10 infrared spectrophotometer.

2.2 PREPARATION OF $Li_2B_{10}Cl_{10}$ AND $Li_2B_{12}Cl_{12}$

The starting materials for $B_{10}Cl_{10}Cl_{10}^{2-}$ were decaborane (Callery Chemical Co.), xylene (Fisher), and triethylamine (Eastman). The process used was originally reported by Hawthorne and Pilling (13). 90g (736 mm) of decaborane were dissolved in 900 ml of xylene, and 270 ml of triethylamine (1,929 mm) were added slowly with stirring. The solution was heated to 100°C with stirring for 3 hrs, then heated to 135°C for 5 hrs. The white precipitate $(NEt_3H)_2B_{10}H_{10}$ was filtered, washed with Fisher isopropyl alcohol, and vacuum dried. The yield was 222g (688 mm) or 93.5% based on decaborane. The amine was removed with a cooled solution of 100g of NaOH (2.75 moles) in one liter of water. Triethylamine was removed with a separatory funnel, and the remaining dissolved amine extracted four times with an equal volume of toluene. The toluene was cycled against an equal volume of water containing 126 ml of 12M hydrochloric acid (1.51 moles). This solution was saved. The aqueous solution containing $B_{10}H_{10}^{2-}$ was slowly acidified with 86.5 ml of glacial acetic acid (1.51 moles) and diluted to 3500 ml in a five liter round-bottom flask. The flask was cooled to 0°C and treated with chlorine gas (Matheson). When the solution acquired a greenish cast, the flask was heated to boiling to remove excess chlorine. The aqueous triethylammonium chloride solution saved from the extraction described above was added slowly with stirring. The precipitated salt $(NEt_3H)_2B_{10}Cl_{10}$ was filtered from the solution and carefully washed. It was dissolved in a solution of 106g $LiOH \cdot H_2O$ (2.59 moles) in 550 ml of water, and the amine extracted as described above.

Recovery of $Li_2B_{10}Cl_{10}$ from the aqueous solution was similar to that described in Ref. 20. The solution was acidified with 111 ml of 12M HCl (1.34 moles) and the remaining amine, now as $(NEt_3H)_2B_{10}Cl_{10}$, was removed by filtration. The solution was made basic again by addition of a slight excess of solid LiOH. An equal volume of tetrahydrofuran (Apache Chemicals) was equilibrated with the solution and separated. Subsequent smaller portions of ether were used until aliquots from the aqueous phase no longer gave a precipitate with aqueous $(NEt_3H)Cl$. The etherial phase was treated with solid LiCl, which caused the separation of an aqueous phase. This was removed as it was formed. The process was continued until the solution was in equilibrium with solid LiCl. The etherial phase was placed in a distillation apparatus with a Berl saddle column and fractionated. The distillate was saved, and fresh dry tetrahydrofuran was added to the pot periodically to replace that distilled. Crystals of solvated $Li_2B_{10}Cl_{10}$ formed in the pot. These were removed and washed with dry tetrahydrofuran, then recrystallized from the distillate. The polyhedral borate anion not crystallized as the lithium salt was recovered by steaming the ether off the pot residue with water and precipitating as $(NEt_3H)_2B_{10}Cl_{10}$. The tetrahydrofuran was recycled. $Li_2B_{10}Cl_{10}$ was heated <u>in vacuo</u> at 160°C until it was free of ether and water.

The preparation of $Li_2B_{12}Cl_{12}$ began with the synthesis of the anion $B_{12}H_{12}^{2-}$ from decaborane (Callery Chemical) and triethylamine borane (Aldrich Chemical) according to the method of Miller and Muetterties (14). A mixture was prepared by adding a solution of 30g of $B_{10}H_{14}$ (0.246M) to 79 ml (62.5g or 0.54M) of triethylamine borane, which was then in 10 m/o excess. This solution was added under argon to 240 ml of Laurelscene (ARCO Chemical) at 190°C with stirring over a period of 20 to 30 min. Laurelscene is the trade name of a purified kerosene which is essentially free of olefins and aromatic compounds. As the drops of solution hit the heated kerosene, reaction occurred yielding the bistriethylammonium salt of $B_{12}H_{12}^{2-}$ and hydrogen. The mixture was stirred at 190°C for another 5 to 10 min, then cooled to 50° to 60°C. The solid was filtered and washed free of kerosene with diethyl ether. The crude product typically weighed about 77g, or 90% yield based on decaborane (14).

This material was dissolved in an excess of cold aqueous sodium hydroxide and filtered to remove insoluble byproducts. The triethylamine was then removed by extraction with toluene and the mixture acidified with acetic acid, diluted and chlorinated as described above at atmospheric pressure, 90°C. Extraction and crystallization of $Li_2B_{12}Cl_{12}$ were carried out as described for $Li_2B_{10}Cl_{10}$. Following the second crystallization from tetrahydrofuran, the salt was heated <u>in vacuo</u> on the glass vacuum line to 150° to 200°C.

2.3 PREPARATION OF ELECTROLYTES

1.8M $LiAlCl_4/SOCl_2$ was prepared as follows: 241g of $AlCl_3$ (Fluka, as received) were added to a one-liter flask under dried air (4% r.h.) containing 800 ml of distilled thionyl chloride. A 10% excess (84g, 2 moles) of lithium chloride (Foote), previously dried for 16 hrs at 160°C in vacuo was added and the mixture stirred overnight. Lithium chips were added and the mixture refluxed. As the chips darkened, more were added. Treatment for 12 to 14 hrs afforded a solution essentially free of hydrolysis products (12). The solution was filtered through glass fiber paper into a 1-liter volumetric flask using glassware previously rinsed with dried $SOCl_2$ and brought to the mark. Solutions of $AlCl_3$ can be made free of $AlCl_2OH$ (12) by continued reflux, but lithium chips cannot be used.

$Li_2B_{10}Cl_{10}/SOCl_2$ and $Li_2B_{12}Cl_{12}/SOCl_2$ electrolytes were prepared by directly dissolving an appropriate amount of solute in purified thionyl chloride. The salts must be weighed in the drybox (10 to 50 ppm H_2O) to avoid the absorption of moisture.

2.4 CELLS FOR GALVANOSTATIC MICROPOLARIZATION MEASUREMENTS

The test cells used the same glass configuration as described previously (6-10), and the electrodes were positioned as shown in Figure 1. All electrodes were made of lithium metal that had been rolled between sheets of plastic prior to assembly in order to expose fresh metal surface. The area of the working electrodes was about 2 cm^2. The cells were assembled in the dry room (≦ 4% r.h.). Prior to filling with electrolyte, the cells were rinsed with dry thionyl chloride. After filling, they were evacuated through a stopcock with the electrolyte held frozen in liquid nitrogen. The electrolyte was allowed to thaw to permit it to outgas, refrozen, the cells were reevacuated and then stored at room temperature, 55° or 72°C for periods up to two months.

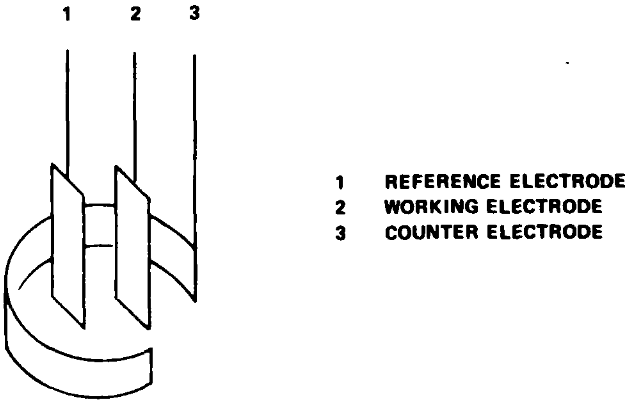

Figure 1. Electrode Configuration for Micropolarization Measurements

After the cells were removed from storage and allowed to cool to room temperature, the potential of the working electrode vs. the reference electrode was monitored as a function of time with a Tektronix type 549 storage oscilloscope triggered by a Princeton Applied Research model 175 Universal Programmer. All measurements were made at room temperature with short pulses of very low constant current to minimize disturbance of the film on the working electrode. These constant current pulses were obtained from the programmer by connecting it in series with a swamping resistor, 100 kΩ or greater, and much larger than the largest total resistance of any cell. Since the programmer output was a constant potential pulse (up to 10V), an essentially constant current pulse was obtained.

Typical storage oscilloscope traces used to calculate the specific capacitance (C) and the specific reaction resistance (R_r) are shown in Figures 2 and 3. Interfacial specific capacitance and solution resistance were calculated from measurements using single 100 μs anodic pulses of 100 μA applied to the working electrode (6), as shown in Figure 2. The initial very rapid rise, if any, reflects the solution resistance.

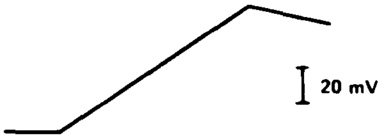

Figure 2. Cell after Ten Days Storage at 25°C Using a 100 μs, 100 μA Pulse. Tracing from a typical storage oscilloscope photograph.

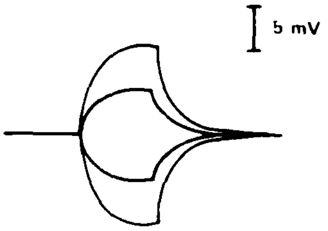

Figure 3. Cell after Ten Days Storage at 25°C on Applying +2, +1, -1 and -2 μA, 10 ms Pulses. Tracing from a typical storage oscilloscope photograph.

The slope of the subsequent trace represents the interfacial specific capacitance of the working electrode (6) according to:

$$C = \frac{i}{(dv/dt)_{t \cdot 0}} \qquad (1)$$

where i is the current density, v the potential, and t the time.

The specific capacitance was used to measure the film thickness (8) according to:

$$d = \frac{\varepsilon}{C \pi 3.6 \times 10^{12}} \tag{2}$$

where ε is the dielectric constant of LiCl. The area of the working electrode was assumed to be the same as the geometric area, while, in fact, the actual area was somewhat larger due to roughness. The values of d found according to this method, therefore, reflect minima, because the minimum areas were used in the calculations. The reaction resistance, R_r, was calculated from the micropolarization of the lithium anode with single 10 ms pulses in steps of one or more microamps, anodic or cathodic, as shown in Figure 3. The resistance of the electrolyte was usually negligible compared with the resistance of the film. The potential of the working vs. the reference electrode was a linear function of the applied constant current, over the time interval of the measurement, and R_r was equal to the slope. The specific resistivity of the film may be found by dividing the reaction resistance by the film thickness.

The measurements described in this and in earlier work are believed to apply to the solid electrolyte interphase only and not to the porous overlayer formed on top of the SEI (6,7).

2.5 PREPARATION OF GLASS AMPOULES USED IN THE ANALYSIS OF LITHIUM CORROSION BY WEIGHT GAIN AND BY SEM OBSERVATION

The ampoules used to measure the weight gain of lithium samples exposed to solvents and electrolytes and to examine lithium samples in the SEM were prepared in the following way. Pieces of lithium foil 2 cm × 6 cm were rolled up with sections of 5-mil thick Crane nonwoven glass fabric and inserted in glass tubes such as diagrammed in Figure 4(a) after exactly 10 ml of the fluid to be tested had already been added to the tube. The tubes were attached to a vacuum line, frozen in liquid nitrogen, and then pumped down. The liquid was permitted to thaw in order to allow any trapped gas to escape, and the tube was once again frozen and evacuated. The tube was then sealed off with a torch as indicated in Figure 4(b), inverted as indicated in Figure 4(c), and stored at the appropriate temperature for the appropriate period of time. When it came time to examine the stored lithium, the ampoules were taken into an argon-filled drybox and broken open where indicated by the arrow in Figure 4(b). Each lithium roll was either carefully unravelled, washed twice with thionyl chloride and weighed after being allowed to dry, or a small piece was sectioned off, washed and mounted for examination under the scanning electron microscope. The samples were transferred to the microscope with the aid of sealed jars and a nitrogen filled antechamber.

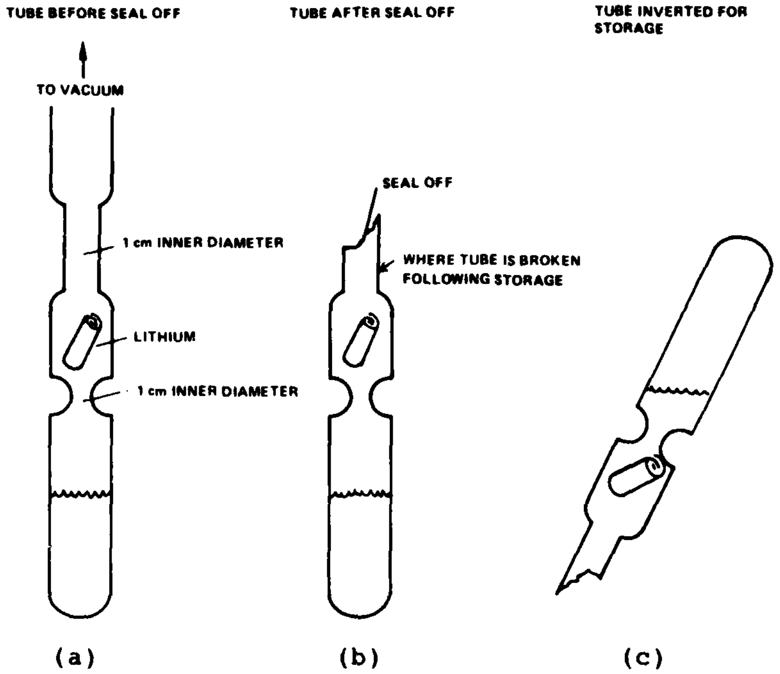

Figure 4. Glass Ampoules for Lithium Corrosion Tests

In all these experiments the ratio of the area of exposed lithium to the electrolyte volume (A/V) was 2.4 cm^{-1} (24/10), which is near that in the cells used for startup and capacity studies (13/4 = 3.25 cm^{-1}). The stored lithium was not in contact with any other metal, eliminating the possibility of self-discharge through local cell reactions.

2.6 PREPARATION OF Li/$SOCl_2$/C AA CELLS

The electrolytes made for this contract were tested in AA-size bobbin cathode type cells. The construction of these cells has been described elsewhere (15). For the work described here, severely anode limited cells were used to compare anode corrosion in $LiAlCl_4/SOCl_2$ with corrosion in the polyhedral borate electrolytes. The anodes were individually weighed, and averaged 0.14g of lithium, while the surface area exposed to the electrolyte was about 13 cm^2.

2.7 INSTRUMENTATION*

Scanning electron micrographs were taken using a JSM-U3 scanning electron microscope manufactured by JEOL. X-ray dispersion analysis was carried out using a Princeton Gamma Tech PGT-1000 X-ray analyzer. It was not calibrated. Visible spectra were taken with reference to air in a 5 mm quartz cell using a Cary 14 recording spectrometer. Electron paramagnetic resonance spectra were taken on an instrument manufactured by Varian.

2.8 ELECTROLYTIC CONDUCTIVITY

The conductivity cell is shown in Figure 5. The capacity of the barrel, with the electrodes in place, was about 25 ml. The polished 19/22 joints were lined with a Teflon sleeve. There was enough volume at the bottom beneath the electrodes for a small magnetic stirring bar. The barrel was fitted with an aluminum collar with fins to aid heat transfer.

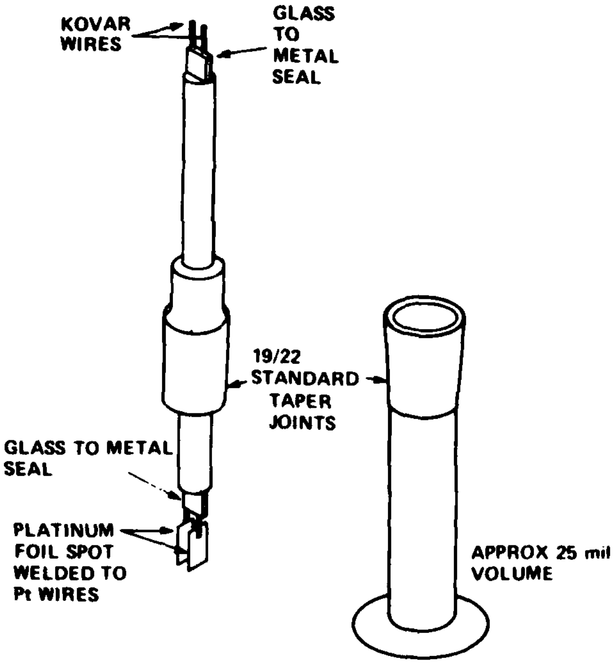

ALL PARTS FABRICATED IN PYREX
EXCEPT AS NOTED

Figure 5. Conductivity Cell

---

*We wish to acknowledge with thanks the SEM photographs prepared by Mr. Kim Ostreicher, GTE Labs; the visible spectra prepared by Mr. Frank Kochanek and Mr. Paul Markatos, also of GTE Labs; and the EPR spectra, taken by Dr. Hans van Willigen of the University of Massachusetts, Boston.

An iron/constantan thermocouple was positioned inside the collar. The assembly with magnetic stirrer and ring stand was placed inside a Blue M model TC40-34X chamber with a small fan to keep the temperature uniform throughout the volume. The cell was calibrated before every run using 0.1 molar aqueous potsssium chloride. Resistance readings were taken using a General Radio model 1656 impedance bridge with square wave excitation from 1 to 4 kHz, and a Tektronix oscilloscope. Readings were taken starting at about +55°C, cooling 10°C at a time, equilibrating 1 to 2 hrs, then reading again. The minimum temperature was about -60°C. Readings were then taken during successively higher temperatures, from -60°C back up to +55°C.

3. RESULTS AND DISCUSSION

3.1 FILM THICKNESS AND RESISTIVITY AS MEASURED BY MICROPOLARIZATION

3.1.1 Micropolarization of Lithium in 1.8M $LiAlCl_4/SOCl_2$

Many of the earlier studies concerning the delay problem used $Li/SOCl_2C$ cells which were started at relatively high current density, anodizing the lithium until the passivating film was essentially separated from the metal (2,3). While this test is more closely related to the problem as it would be encountered by a customer's attempting to use the cells, several disadvantages are apparent. The method is destructive, and cells cannot be used for tests following further storage. The result is only qualitative, and duplicate cells often do not show similar characteristics (3,17). Such test cells do not have reference electrodes, and polarization due to anode passivation is often confounded with cathode polarization. The pulse technique offers solutions to all of these problems.

The minimum thickness, d_{min}, is plotted against storage time at three different temperatures for six different cells in Figure 6. The reaction resistance for the same cells is plotted vs. time in Figure 7.

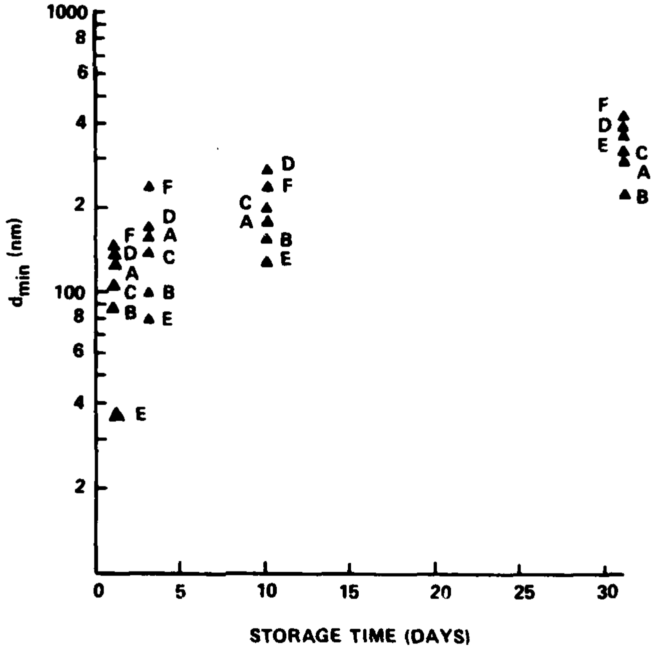

Figure 6. d_{min} as a Function of Time and Storage Temperature. Cells A, B stored at 25°C; C, D at 55°C; E, F at 72°C. 1.8M $LiAlCl_4/SOCl_2$.

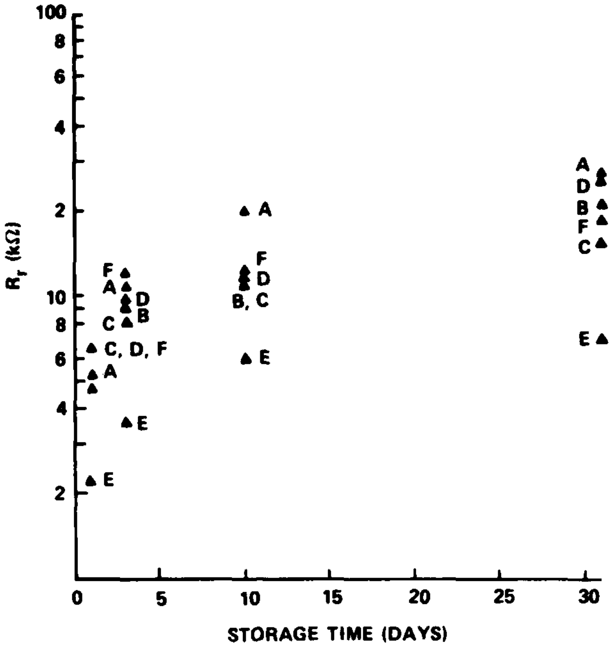

Figure 7. R_r as a Function of Time and Storage Temperature. For temperatures see Figure 6. 1.8M $LiAlCl_4/SOCl_2$.

The values of R_r and d_{min} found here are somewhat higher than those previously reported (7,8), although some scatter was noted in the data. Reproducibility in the measurement of R_r and d_{min} is important if any meaningful comparisons of film growth rates are to be made between electrolytes prepared using $LiAlCl_4$ and those prepared using $Li_2B_{10}Cl_{10}$ or $Li_2B_{12}Cl_{12}$. We noted that our procedure for refluxing of electrolytes was not carried out during the course of the previous investigations. Although our reason for refluxing the electrolytes in the presence of lithium was to remove hydrolysis products, excess aluminum chloride may also have been removed during refluxing. For this reason an additional cell was constructed, and a sufficient amount of solution of $AlCl_3$ in $SOCl_2$, dried by refluxing without lithium, was added to the electrolyte to make to concentration 10^{-3} molar in excess aluminum chloride. The cell was stored at room temperature, as were cells A and B. The thickness d_{min} for the new cell as a function of time is compared with d_{min} for cells A and B in Figure 8, while the reaction resistance is compared in Figure 9. Both were found to be lower.

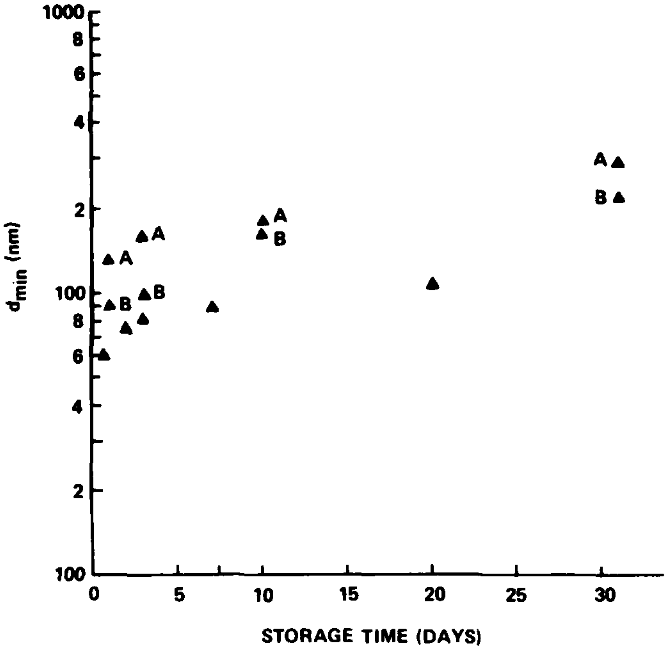

Figure 8. d_{min} as a Function of Time Stored at Room Temperature. Unlabeled points correspond to the cell with added $AlCl_3$.

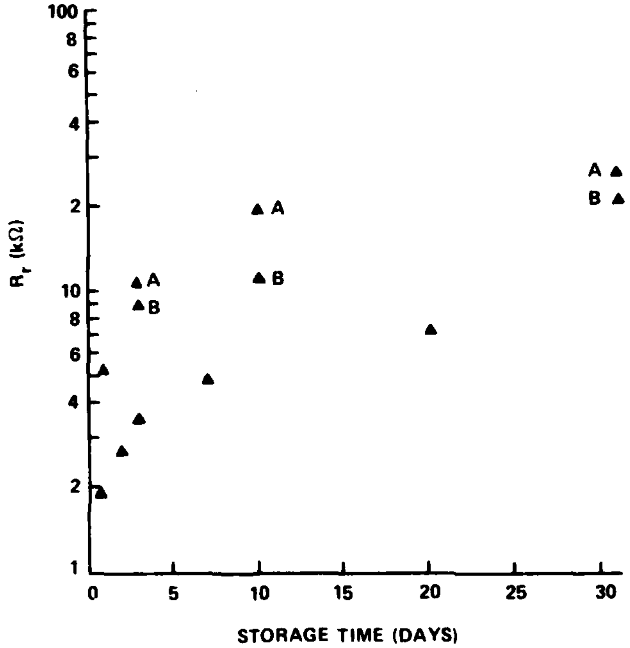

Figure 9. R_r as a Function of Time Stored At Room Temperature. Unlabeled points correspond to the cell with added $AlCl_3$.

The purposeful addition of excess $AlCl_3$ to electrolyte in order to reduce voltage delay has been discussed by Marincic and Lombardi (3,16). In their experiments, aluminum chloride was present in the solution at 10 m/o greater than the amount of lithium chloride. At this level, the aluminum chloride was found to be highly corrosive of the lithium. It is not known what concentration of aluminum chloride remains in 1.8M $LiAlCl_4$ which has not been refluxed following the addition of excess solid lithium chloride, but it is clear that minute concentrations of $AlCl_3$ will affect the rate and extent of film growth.

Alleviation of the voltage delay problem by the addition of excess $AlCl_3$ offers two disadvantages. First, the effect cannot be a lasting one, since $AlCl_3$ is used up in the process of removing the film; second, anode corrosion and loss of solvent by reduction occur. Therefore, addition of more $AlCl_3$ to increase the time interval over which it will effectively remove the film is self-defeating, since the shelf life is reduced. We do not recommend pursuing this technique for reducing the voltage delay.

Examination of the film by these techniques has revealed that storage temperature did not significantly affect the growth rate or the reaction resistance when these were measured at room temperature. Since the voltage delay in $Li/SOCl_2$ cells had been found to worsen by storage at elevated temperature, the connection between the delay and the electrical properties of the film as proposed by the SEI model was not clear. Therefore, the thickness and reaction resistance were measured at the temperatures used to store the samples, as well as at room temperature. All previous measurements had been carried out only at room temperature.

After storage for three months at 55°C, two cells were measured by pulse polarization techniques to determine the minimum film thickness and reaction resistance of the film on each working electrode before and after cooling to room temperature. The results are shown in Table 1.

According to the data and the SEI model, the LiCl layer was more conductive at 55°C than at 28°C, and the film thickness was not substantially different whether measured at 55° or 28°C. The specific resistivity was significantly lower at the higher temperature, which might reflect the higher conductivity known to occur in solid salts at higher temperature. For these calculations, the dielectric constant of solid LiCl was assumed to be the same at both temperatures. It is also reasonable to expect that the thickness of the LiCl films should not change during the relatively short period of time required to cool the cells. The measurements were consistent with this premise.

TABLE 1

SOLID ELECTROLYTE INTERPHASE THICKNESS AND RESISTIVITY AT 28° AND 55°C

Cell No.	Parameter	28°C	55°C
42C	d_{min}	4.2×10^2 nm	3.3×10^2 nm
	R_r	25 kΩ	10.7 kΩ
	Specific Resistivity	5.5×10^8 Ω-cm	3.3×10^8 Ω-cm
42C	d_{min}	5.8×10^2 nm	5.5×10^2 nm
	R_r	38.6 kΩ	23.6 kΩ
	Specific Resistivity	6.7×10^8 Ω-cm	4.2×10^8 Ω-cm

3.1.2 Effect of the Lithium Area to Electrolyte Volume Ratio on the Properties of LiCl Films on Lithium in $SOCl_2$ with Tetrachloroaluminate

The quotient A/V, or the ratio of the area of exposed lithium to the volume of solvent or electrolyte, has been observed to influence gassing rates in corrosion tests using organic solvents (18,19). It was observed that the greater the A/V ratio, the greater the amount of gassing (19). If the gassing had been caused by reaction of Li with dissolved water, the amount of gas should have been dependent only on the volume, which is directly proportional to the concentration of dissolved impurity. The conclusion was that the lithium was reacting directly with the solvent through a catalytic mechanism involving the impurity. The possibility exists that a similar mechanism occurs in the $Li/SOCl_2$ system. In Figure 6, where d_{min} is plotted and in Figure 7, where the reaction resistance is plotted as a function of time, cell E shows a lower film thickness and reaction resistance than expected, considering the storage temperature. The area of the working electrode was less, although the electrolyte volume was about the same as in all the other cells. Variation in the ratio of A to V in our test cells was small enough that any effect on film growth rate was lost in experimental uncertainty except for the two cells stored at 72°C. The ratios of A to V for these cells are compared with values of d_{min} in Table 2. When A/V was greater the measured film was significantly thicker.

The results shown in Table 2 reinforce the possibility that soluble products resulting from corrosion catalize further lithium corrosion and film building or gassing reactions (autocatalysis). For a given rate of reaction of the solvent or electroltye with a unit area of lithium, the concentration of soluble products resulting from lithium corrosion and film formation would be higher if the ratio of surface area to liquid volume were higher. The higher concentration of these products, if they influenced the rate by a catalytic mechanism, would then cause faster film growth.

TABLE 2

COMPARISON OF THE A/V RATIOS WITH THE VALUES OF d_{min}

Cell No.	A/V (cm^{-1})	d_{min} after Storage at 72°C (× 10^2 nm)			
		1 Day	3 Days	10 Days	31 Days
42E	0.138	0.35	0.81	1.3	3.6
42F	0.96	1.5	2.4	2.4	4.1

An analogous effect has been observed for voltage delay in different types of cells, as shown in Table 3.

The A/V ratio in wound "D" cells is greater than the A/V ratio in AA cells, and wound "D" cells experience a more significant delay problem. As discussed below, corrosion of lithium may also be affected by the exchange of lithium chloride from the passivating film with lithium chloride present in solution. If the ratio of the area of lithium to the volume of electrolyte is larger, the concentration in solution may be larger, causing a more rapid exchange. The more rapid exchange would be disruptive of the film, causing displacement of the lithium chloride and more extensive lithium corrosion.

TABLE 3

VOLTAGE DELAY AS A FUNCTION OF CELL CONSTRUCTION

Cell Type	Current Density (mA/cm^2)	Time to Minimum Potential (s)	Minimum Potential (V)	Time to 3V (s)	Volts at 30s	Storage Time (Days)
AA*	0.75	1	2.97	0.35	3.25	38
Wound D**	1	1	2.5	3	3.1	30

*Average of four cells; a fifth cell did not delay.

**From Figure 5, Ref. 17.

3.1.3 0.25M $Li_2B_{10}Cl_{10}$: Micropolarization of Lithium Samples and Comparison with $LiAlCl_4/SOCl_2$

The thickness (d_{min}) of the chemically passivating film, calculated as described above, is shown as a function of storage time for representative electrodes in 1.8M $LiAlCl_4/SOCl_2$ and 0.25M $Li_2B_{10}Cl_{10}$ at room temperature (Figure 10), and at 55°C (Figure 11). After 30 days the film on the electrode stored at 25°C in 0.25M $Li_2B_{10}Cl_{10}$ was about 1/5 as thick, while at 55°C it was about 1/3 as thick. The film also did not appear to continue growing as fast after the first three or four days, in contrast to $LiAlCl_4$ where the film continued to grow for a month or more. The film thickness was found to be more strongly temperature dependent in the boron electrolyte, being twice as great after 30 days at 55°C than at 25°C.

The reaction resistance (R_r) of the film on lithium electrodes stored at room temperature in 0.25M $Li_2B_{10}Cl_{10}/SOCl_2$ was two orders of magnitude less than in 1.8M $LiAlCl_4/SOCl_2$, as shown in Figures 12 and 13. The reaction resistance of the film found in the boron electrolyte was also more strongly dependent on the storage temperature than it was in the aluminum electrolyte. For example, in Figure 13, the reaction resistance after 10 days at 55°C was over six times that produced at room temperature, while in Figure 7, raising the storage temperature from 25° to 55°C did not significantly affect the reaction resistance in 1.8M $LiAlCl_4$.

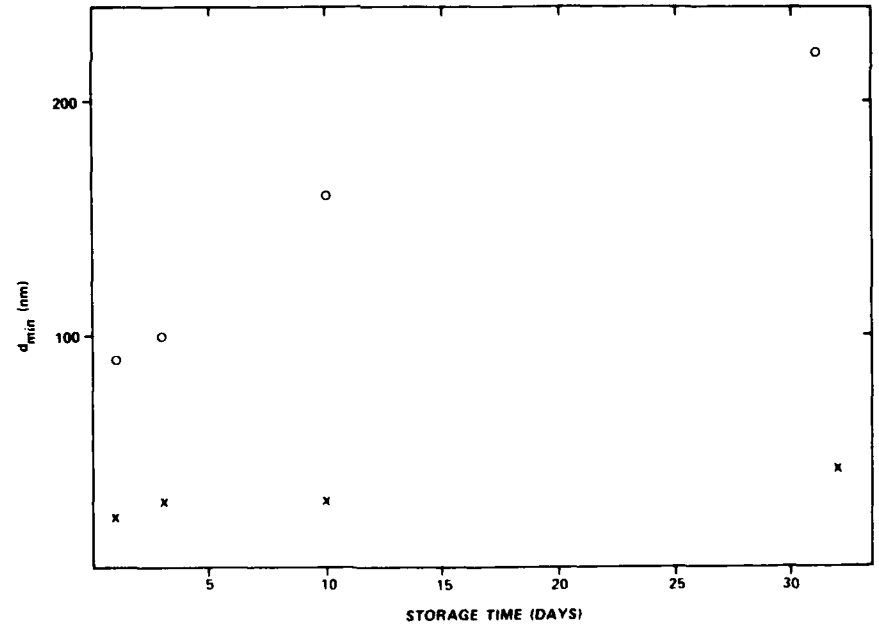

Figure 10. d_{min} for Representative Lithium Electrodes Immersed in 0.25M $Li_2B_{10}C_{10}/SOCl_2$ (X) and 1.8M $LiAlCl_4/SOCl_2$ (O) Stored at Room Temperature

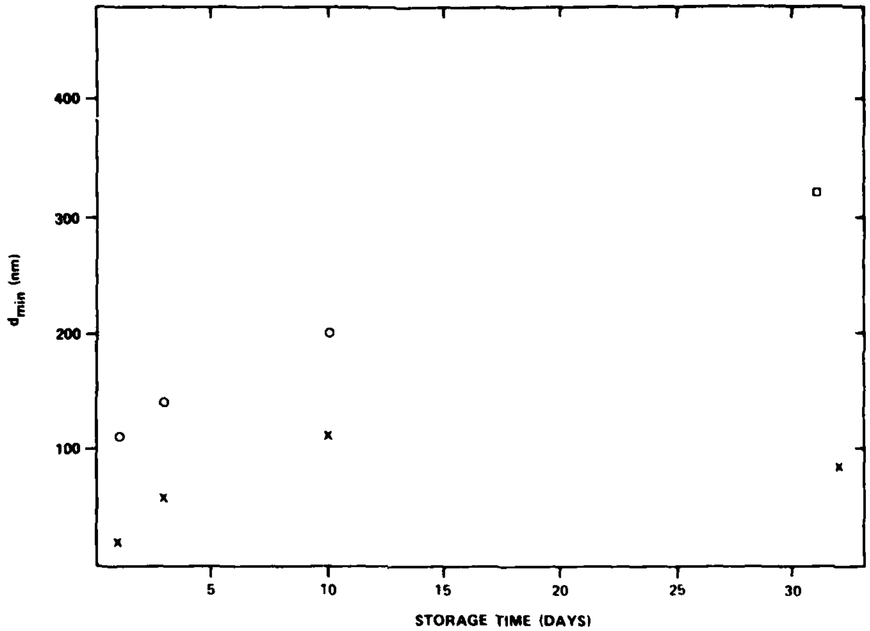

Figure 11. d_{min} for Representative Lithium Electrodes Immersed in 0.25M $Li_2B_{10}Cl_{10}$ (X) and 1.8M $LiAlCl_4$ (O) Stored at 55°C

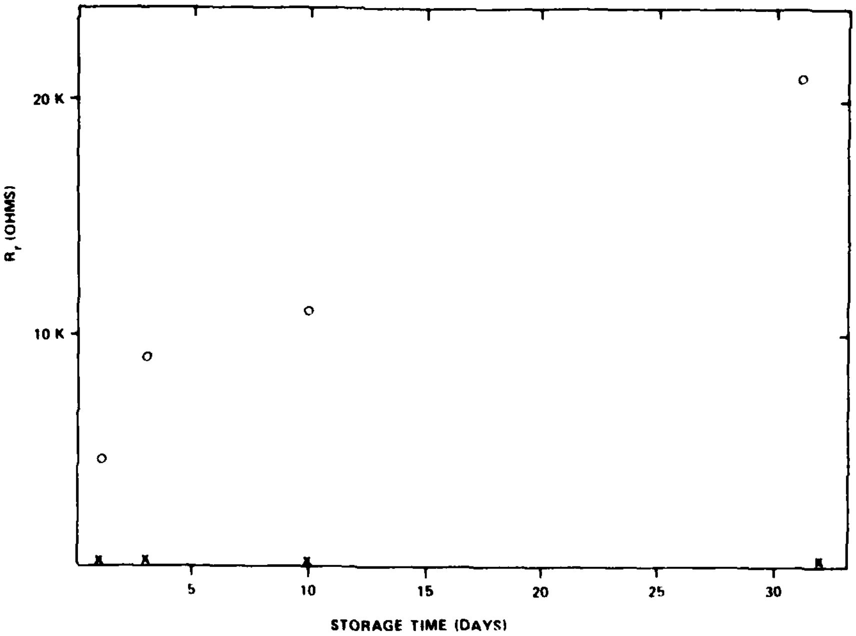

Figure 12. R_r for Representative Lithium Electrodes Immersed in 0.25M $Li_2B_{10}Cl_{10}/SOCl_2$ (X) and 1.8M $LiAlCl_4/SOCl_2$ (O) Stored at Room Temperature

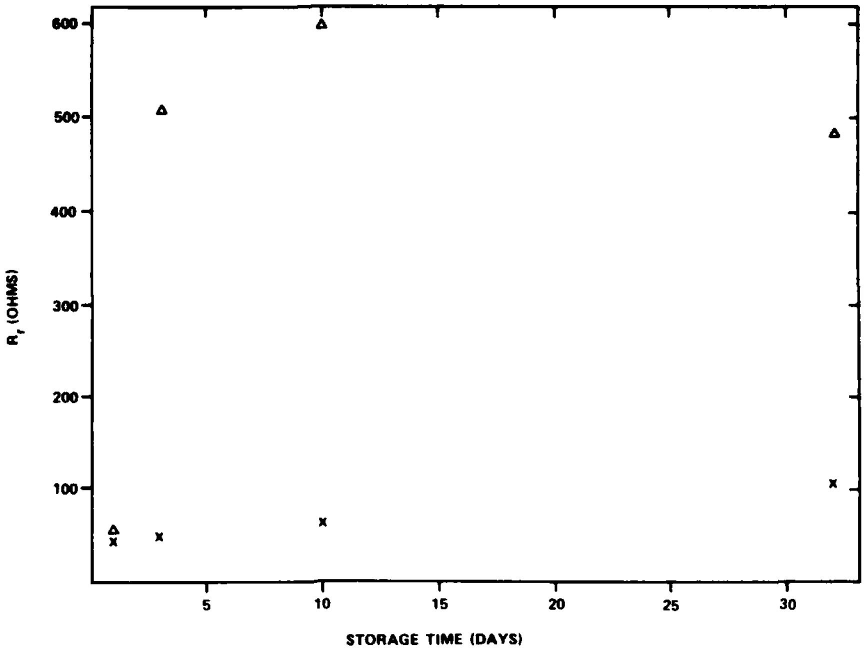

Figure 13. R_r for Representative Lithium Electrodes Immersed in 0.25M $Li_2B_{10}Cl_{10}$ Stored at Room Temperature (X) and 55°C (Δ)

Differences in the concentration of lithium between the two electrolytes cannot account for the differences in d_{min} and R_r, since Peled found less variation in d_{min} and R_r by changing the concentration of $LiAlCl_4$ (21) than we have observed by changing the electrolyte salt. The specific resistivity of the film formed in the borate electrolyte at 25°C after 30 days was about 2.63×10^7 Ω cm, while at 55°C, it was 6.00×10^7 Ω cm, measured after cooling to room temperature. The specific resistivity of the chemically passivating layer found in $LiAlCl_4$ at 25°C from Figures 10 and 12, was 93.6×10^7, and shown in Table 1, 67×10^7 Ω cm. The borate electrolyte was therefore found to affect substantially the specific resistivity of the chemically passivating film, reducing it by about a factor of 30.

3.1.4 Micropolarization of Lithium in $Li_2B_{12}Cl_{12}/SOCl_2$

The film thickness and reaction resistance were calculated as described above for lithium electrodes immersed in 0.23M $Li_2B_{12}Cl_{12}$. The film thickness is shown in Figure 14 as a function of time and temperature for six different lithium working electrodes. The value of d_{min} did not further increase after a few days at room temperature, but continued to rise for the electrodes stored at 55°C. Values of R_r behaved in a similar manner, but for electrodes stored at 55°C, were scattered over almost a factor of 10. Typically after 22 days, R_r was less than 2000Ω for electrodes stored at room temperature, but for electrodes stored at 55°C, R_r had risen to values between 1000Ω and 9000Ω after 13 days.

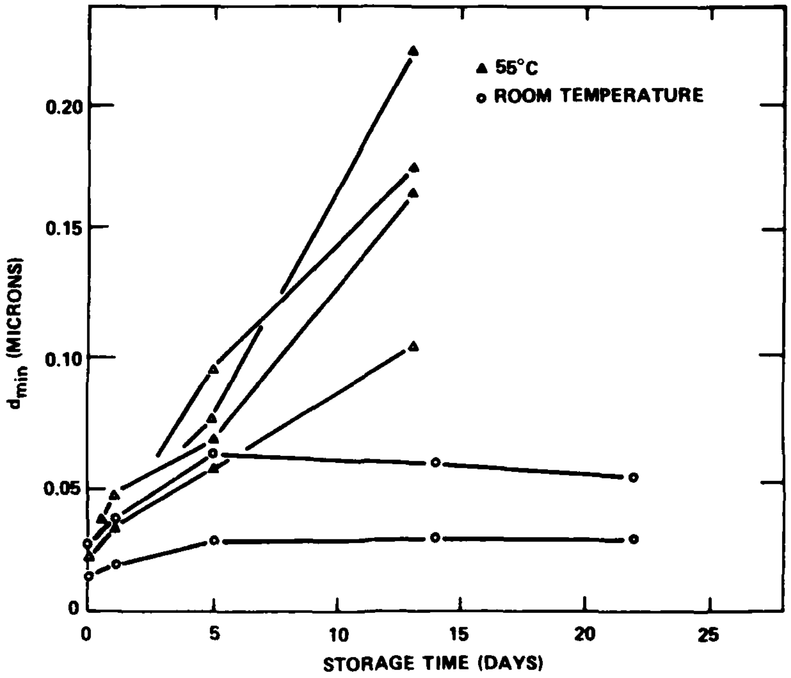

Figure 14. d_{min} as a Function of Time and Temperature for Lithium Electrodes in 0.23M $Li_2B_{12}Cl_{12}/SOCl_2$

3.2 FILM GROWTH AS MEASURED BY WEIGHT GAIN, AND MORPHOLOGY AS OBSERVED BY SEM

3.2.1 Film Growth in Pure $SOCl_2$

To establish the validity of our experimental approach, scanning electron micrographs were taken of an untreated lithium surface as received from the manufacturer. Tool marks from the lithium foil extruder were found, but no obvious pitting or corrosion were present. After momentary exposure to thionyl chloride, a lithium sample examined at a magnification of 300X showed the same tool marks with a hazy film covering the surface. Washing the sample with $SOCl_2$ had not physically altered the lithium, nor had the technique introduced features not originally present (40).

The film thickness and the depth to which the lithium was corroded have been calculated assuming that all of the weight gain corresponded to a completely adherent layer of pure lithium chloride, and that none of it dissolved in the electrolyte. These numbers (in microns) are entered in all figures showing weight gains. The slight solubility of LiCl may have caused attrition, or dissolution from the film and crystallization elsewhere, as on the sides of the glass ampoules. If any attrition occurred, or if the coating was not pure lithium chloride, the calculated thicknesses have been affected. The measurements are meant primarily to provide comparisons between storage under different conditions and an estimation of the average film thickness after storage.

In Figure 15, the weight gains of lithium samples immersed in pure $SOCl_2$ are plotted as a function of time and temperature. The weight gain was small and the uncertainty in the measurement caused scatter in the data. On the basis of these experiments, the storage temperature did not appear to have significantly altered the extent of corrosion.

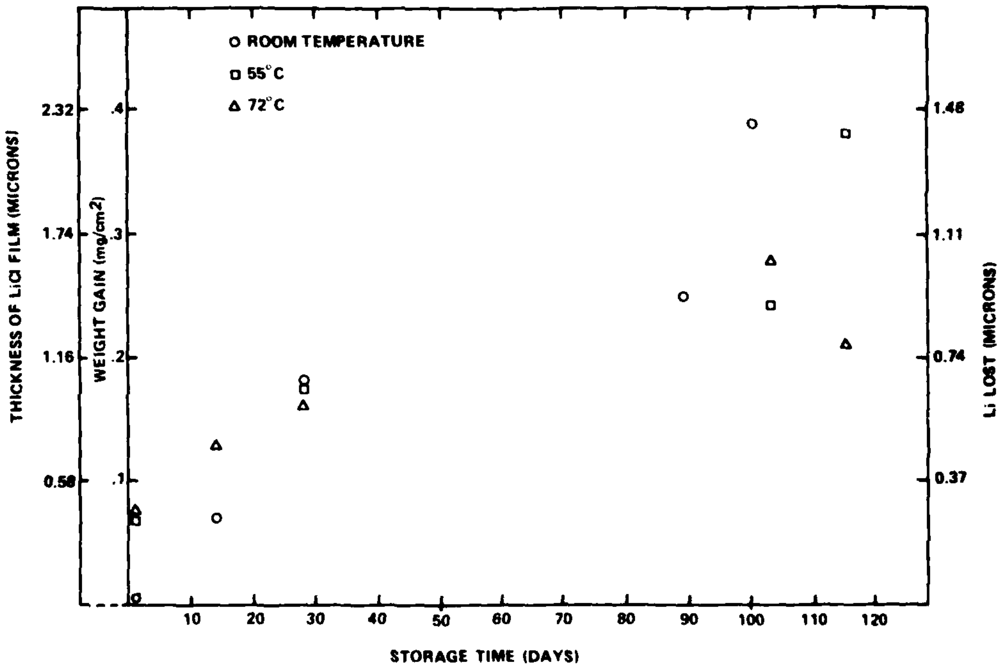

Figure 15. Weight Gain for Lithium Samples Stored in Sealed Ampoules of $SOCl_2$

When lithium samples stored at room temperature in thionyl chloride were examined under the scanning electron microscope (SEM), no crystals were observed after periods up to 59 days. The lithium, when examined after 59 days at a magnification of 1,000X, showed a smooth surface marred by amorphous growths spaced irregularly and along cracks. At 10,000X magnification, the areas devoid of growths appeared irregular and amorphous (40).

Lithium samples stored at 55°C in pure thionyl chloride, when examined after 25 days at 1,000X magnification, revealed a surface similar to that observed for samples stored at room temperature, described above. When examined at 3,000X after 80 days at 55°C, the surface was completely covered by what appeared to be crystalline material overlain with a rough coating. The average crystal diameter was about 3000 nm (3 μm).

Lithium stored at 72°C in pure thionyl chloride was examined after 25 days and after 83 days. After 25 days, the surface at 1,000X magnification appeared smooth with irregularly spaced growths, similar to the surface found at room temperature. Under high magnification at 10,000X, the surface showed a uniform layer of crystals about 0.4 to 0.6 μm in diameter. After 83 days, the largest crystals, now fairly well formed, had grown to about 9 μm with a wide range of sizes down to about 1 μm (40).

Crystallinity had developed in the chemically passivating film on the lithium samples, with the larger, more definite crystals growing at the higher storage temperatures or during the longer periods of storage time. Materials separating out as solids from liquid solutions usually produce crystals with larger crystals forming if the rate of growth is slower or if the solubility is higher. The small but finite solubility of lithium chloride in thionyl chloride, which likely increases with temperature, probably influenced the formation of crystalline as opposed to noncrystalline films on the lithium surface.

Lithium metal samples stored in pure thionyl chloride, when analyzed by x-ray energy dispersion spectrometry, were found to contain sulfur as well as chlorine. Samples stored in $LiAlCl_4/SOCl_2$ were previously reported to develop films containing only chlorine (1). The analytical method can detect elements heavier than sodium on the surface of specific areas of fields observed with the SEM. The composition of material beneath the surface does not affect the measurement. In the sample stored at room temperature for 50 days, discussed above, chloride and some sulfur were detected in the smooth areas. The ratio of the peak heights was consistent over the smooth areas. In the localized areas of more extensive corrosion containing amorphous growths, peak heights were inconsistent, but usually contained more sulfur than the smooth areas. X-ray dispersion analysis of the crystals on the surface of the lithium stored at 72°C for 83 days revealed only chlorine. The smoother areas between these crystals contained sulfur. It is possible that the first rapid film-forming reactions on lithium placed in $LiAlCl_4/SOCl_2$ could produce a passivating film nearest the lithium metal which contains a mixture of more strongly reduced species, including sulfur compounds as well as lithium chloride.

3.2.2 Film Growth in 1.8M $LiAlCl_4/SOCl_2$: Comparison with Micropolarization Measurements

The surface morphology of lithium samples exposed briefly to 1.8M $LiAlCl_4/SOCl_2$ and rinsed with pure thionyl chloride did not differ noticeably from morphology observed on lithium exposed only to thionyl chloride when both were examined at the same magnification between 300 and 1,000 times. In Figure 16, the growth rate in pure $SOCl_2$ is compared with the rate in 1.8M $LiAlCl_4/SOCl_2$, when samples were stored at 72°C for periods up to one month. The rate of film growth was substantially greater in the solution containing $LiAlCl_4$, indicating that the presence of $LiAlCl_4$ aggravated the corrosion of the lithium. The thickness of the film as a function of time, calculated from the weight gain measurements, is shown in Figure 17 for storage in 1.8M $LiAlCl_4/SOCl_2$ at ambient temperature, 55° and 72°C. The rate of film growth was higher as the temperature was increased.

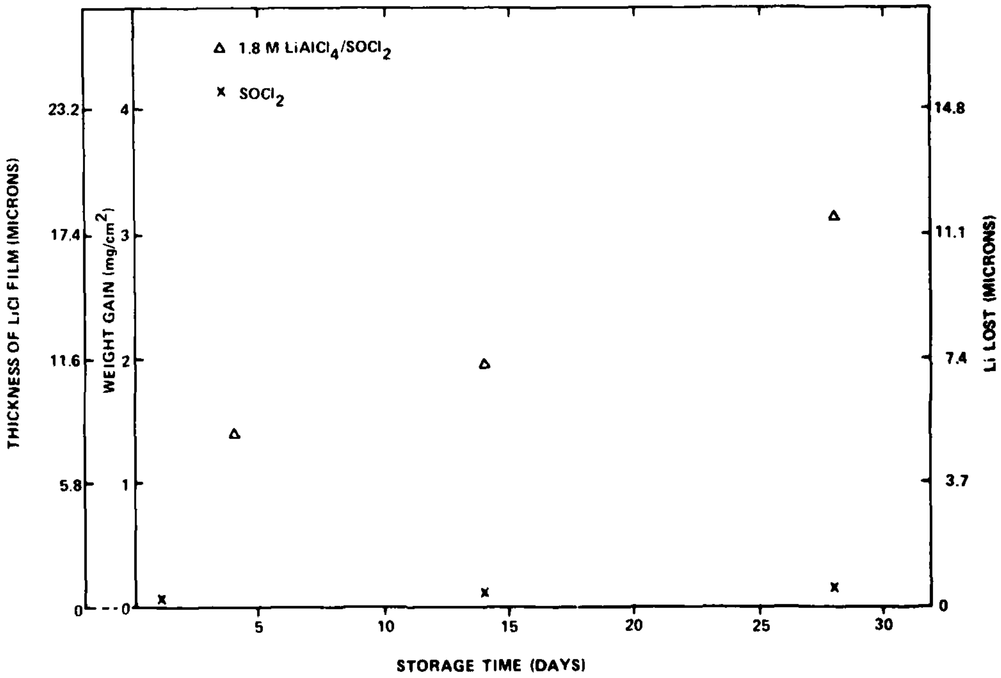

Figure 16. Weight Gain of Lithium Samples Stored in Sealed Ampoules at 72°C

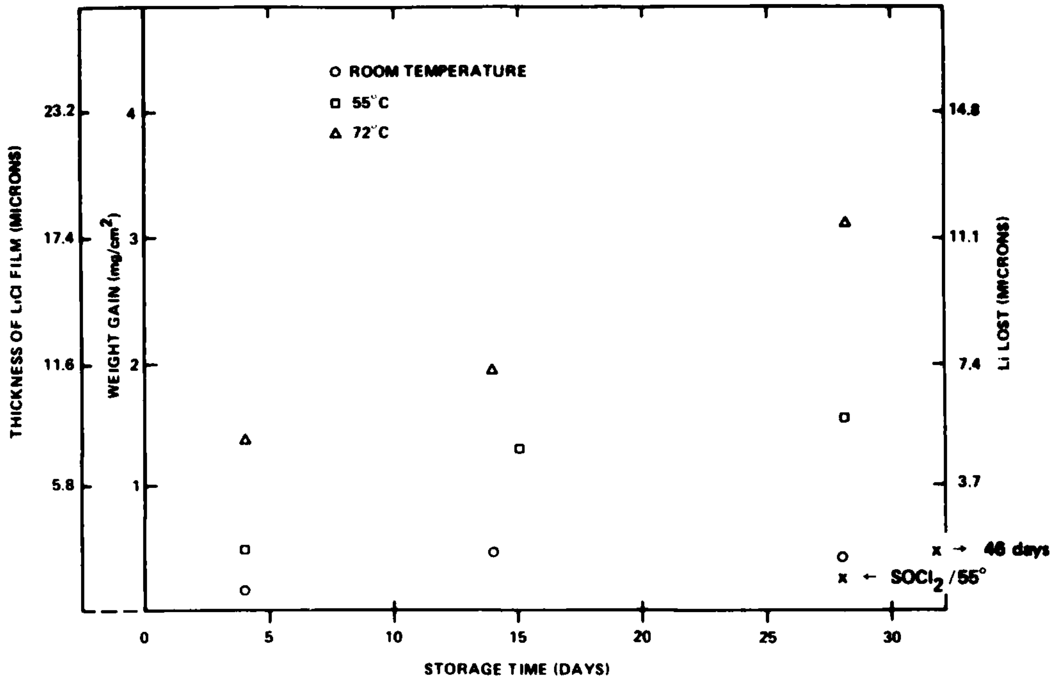

Figure 17. Weight Gain of Lithium Samples Stored in Sealed Ampoules of 1.8M $LiAlCl_4/SOCl_2$

The logarithm of the total film thickness measured by weight gain and the film thickness calculated with capacitance obtained from micropolarization measurements are compared as a function of storage time in Figure 18. Calculations based on micropolarization measurements indicated that the average thickness was less than 0.5 μm after 30 days at room temperature or at 72°C. Weight gain measurements indicated that the thickness after 30 days was 2.5 μm (room temperature) or about 18 μm (72°C). The results are generally consistent with previous data concerning the thickness of passivating films as measured by each of these techniques. The electrical measurement relates to the part of the film which completely covers the lithium, since the porous overlayer, although it contributes to most of the weight, conducts primarily by transport through the liquid electrolyte contained within the overlayer. The chemically passivating film, or solid electrolyte interphase, was also previously found to constitute only about 1% to 10% of the total film thickness (21).

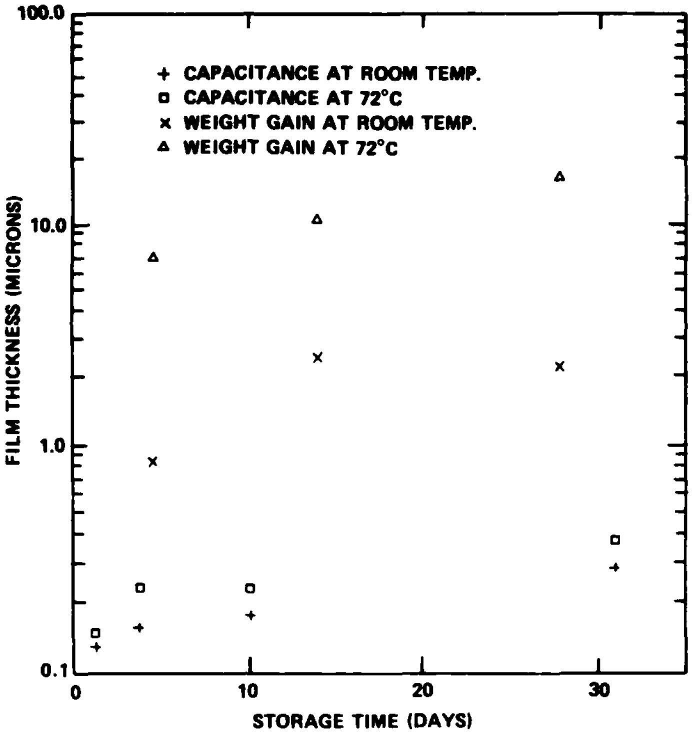

Figure 18. Film Thickness Measured by Capacitance and by Weight Gain. Lithium metal stored in 1.8M $LiAlCl_4/SOCl_2$.

Scanning electron micrographs of lithium samples stored in 1.8M $LiAlCl_4SOCl_2$ at room temperature, 55° and 72°C were taken over a period of about ten weeks. After one day at 72°C, a layer of crystals averaging about 5 μm in diameter completely covered the surface, as shown in Figure 19. After 17 days at 55° or 72°C, the crystals ranged from 3 to 30 μm in diameter, with the average size slightly larger for samples stored at 72°C (40). The average diameter of the crystals did not appear to change appreciably between 17 days and 73 days, while the range of crystal diameters remained large. Crystals on samples stored at 55°C looked consistently cubic, while at 72°C, more facets developed in the cubic lithium chloride. Samples stored at room temperature acquired a uniform layer of crystals within one day of storage, which grew to an average size of about 1 μm after 17 days. The crystals continued to grow and averaged about 5.7 μm after 73 days (Figure 20). The average diameter of the crystals visible on the surface of these samples is consistent with the film thickness measured by weight gain in that the values were roughly equivalent.

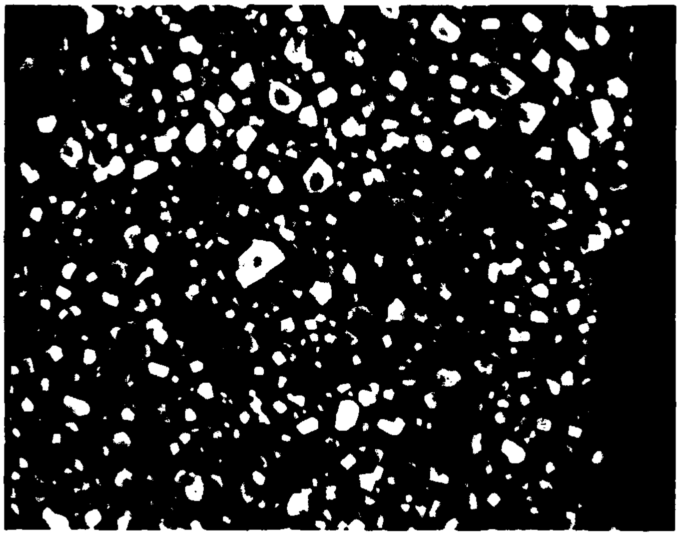

Figure 19. SEM of Lithium Surface Exposed to 1.8M $LiAlCl_4/SOCl_2$ for One Day at 72°C, 1000X

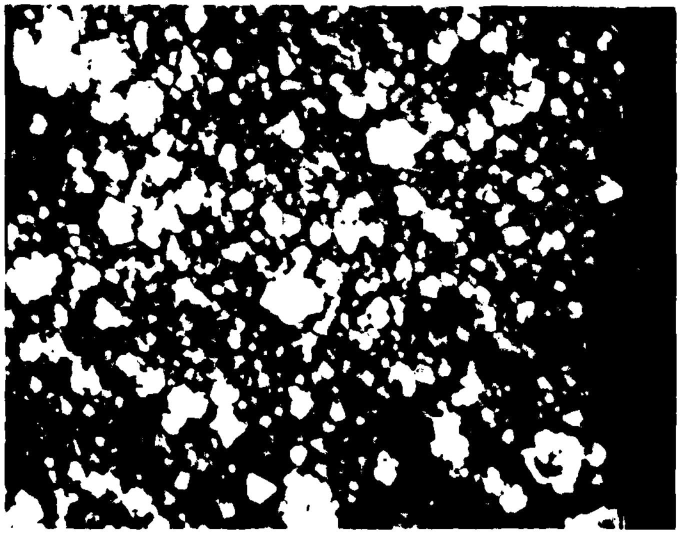

Figure 20. SEM of Lithium Surface Exposed to 1.8M $LiAlCl_4/SOCl_2$ for 73 Days at Room Temperature, 1000X

These results may be compared with the growth of LiCl crystals on lithium stored in thionyl chloride alone, as discussed above. The increased temperature of storage, having produced larger crystals on the lithium surface, probably did so by increasing the solubility of lithium chloride in the electrolyte or by causing faster exchange of solid with dissolved salt. The presence of crystals on samples stored at room temperature in $LiAlCl_4/SOCl_2$ may indicate that the solubility of LiCl is higher, or the exchange of solid with dissolved salt is faster than in pure thionyl chloride at room temperature. The exchange could occur through reversible dissociation of tetrachloroaluminate, as follows:

$$Li^+ \; AlCl_4^- \rightleftarrows \underline{LiCl} + AlCl_3$$

Increased solubility or exchange of solid lithium chloride with the solution could cause greater corrosion of the lithium surface, since dissolution of LiCl would be expected to occur on the thin solid electrolyte interphase as well as on other lithium chloride surfaces, allowing direct reaction of the metal with the solvent.

3.2.3 Film Growth in 0.25M $Li_2B_{10}Cl_{10}/SOCl_2$

Even momentary exposure of lithium metal to 0.25M $Li_2B_{10}Cl_{10}/SOCl_2$ at room temperature resulted in the development of a film and chemical passivation. The surface of a piece of lithium immersed in this electrolyte, then rinsed with thionyl chloride to remove the polyhedral borate salt, showed the original tool markings to be still present, but coated with a thin haze (40).

Scanning electron micrographs were taken of lithium samples stored for 19 days in 0.25M $Li_2B_{10}C_{10}/SOCl_2$ at ambient temperature (Figure 21) and at 55°C (Figure 22). For both samples, the lithium was found to be covered by a smooth passivating layer, with cubic crystals scattered over the surface. The smooth areas, much smoother than the original lithium, are believed to be a coating of salt, since the sample stored at room temperature developed cracks when flexed during mounting (Figure 21). The smooth layer appeared much darker than the crystals, indicating that the layer was more conductive. It was therefore likely compact and closely adherent to the metal, while the tops of the crystals were light in color because of their limited conductivity and remoteness from the surface. Analysis of the smooth areas by EDAX found that chloride was present, but no sulfur. A different technique such as ESCA will be required to determine whether such films contain lithium or boron. The cubic crystals on the room temperature sample ranged from 0.3 to 0.4 μm; average size, about 1.7 μm. The sample stored at 55°C had many more of the cubic crystals, average size about 8 μm, interspersed with crystalline needles, which protruded from the surface.

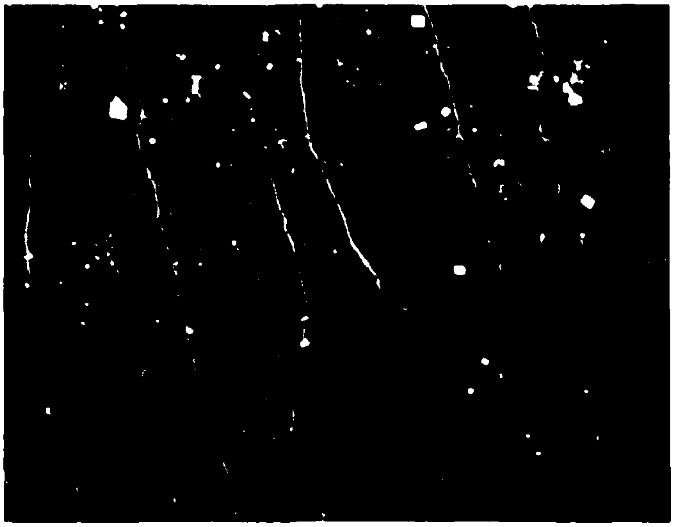

Figure 21. SEM of Lithium Surface Stored at Room Temperature for 19 Days in 0.25M $Li_2B_{10}Cl_{10}/SOCl_2$, 1000X

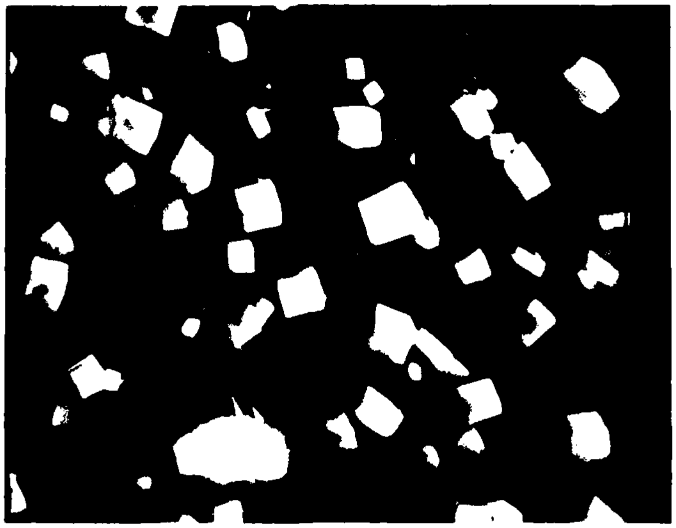

Figure 22. SEM of Lithium Surface Exposed to 0.25M $Li_2B_{10}Cl_{10}$ $SOCl_2$ for 19 Days at 55°C, 1000X

The cubic crystals might have been lithium chloride which had grown from species present in the solution as the result of a reaction between the borate anion and the solvent, rather than from simultaneous corrosion of lithium and solvent reduction. Lithium chloride was found to grow from solutions of $Li_2B_{10}Cl_{10}$ in thionyl chloride (22). To explore this possibility, a piece of glass from the tube in which the lithium had been stored at 55°C was also examined under the SEM. Cubic crystals could be seen on the monitor, but they could not be photographed because of the charge which accumulated on the electrically insulating glass surface.

The extremely smooth chemically passivating surface on lithium stored in these solutions is remarkable and difficult to explain. The random growth of metals such as copper from aqueous solution during electrodeposition or chemical polishing is thought to be responsible for the formation of smooth surfaces (41). The random growth of a film of lithium chloride on lithium in $Li_2B_{10}Cl_{10}/SOCl_2$ might occur as the result of reaction at the surface of the metal without participation of dissolved lithium chloride near the interface. The surface also may lack crystallinity because it consists of a mixture of compounds rather than a single pure substance. It is possible that the smooth layer actually was the solid electrolyte interphase, essentially devoid of an overlayer. The appearance of the needle-shaped crystals was also distinctly different from the behavior of lithium surfaces exposed to $LiAlCl_4/SOCl_2$.

After 69 days of storage at room temperature the number of crystals scattered on the surface of the stored lithium was greater than it had been after 19 days (Figures 21 and 23), and the smooth substrate surface had become rougher when compared at a magnification of 10,000X. The average length of a crystal edge was about 10 μm. After 69 days of storage at 55°C the surface was completely covered with cubic crystals averaging about 8 μm on an edge (Figure 24). The lithium surface stored at room temperature for 69 days (Figure 23) was similar to the one stored at 55°C for 19 days (Figure 22). A sample stored for 8 days at 72°C was completely covered with cubic crystals, showing no smooth undercoating at all (Figure 25). The average crystal diameter was approximately 3.3 μm, with a range from 0.3 to 5.7 μm. EDAX analysis of all these surfaces showed the presence of chlorine, but no sulfur.

The weight gain and calculated film thickness of lithium samples stored in 0.25M $Li_2B_{10}Cl_{10}/SOCl_2$ as a function of time and temperature are plotted in Figure 26. If it is assumed that the gain in weight is due entirely to precipitation caused by solvolysis of the borate anion rather than to lithium corrosion, then the calculated thickness would be 16% less than that indicated in Figure 26. The difference in weight gain between

Figure 23. SEM of Lithium Surface Exposed to 0.25M $Li_2B_{10}Cl_{10}/SOCl_2$ for 69 Days at Room Temperature, 1000X

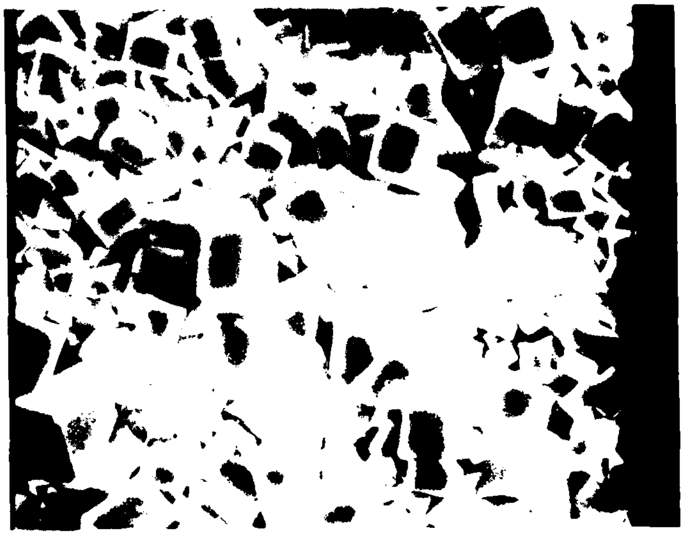

Figure 24. SEM of Lithium Surface Exposed to 0.25M $Li_2B_{10}Cl_{10}$ for 69 Days at 55°C, 1000X

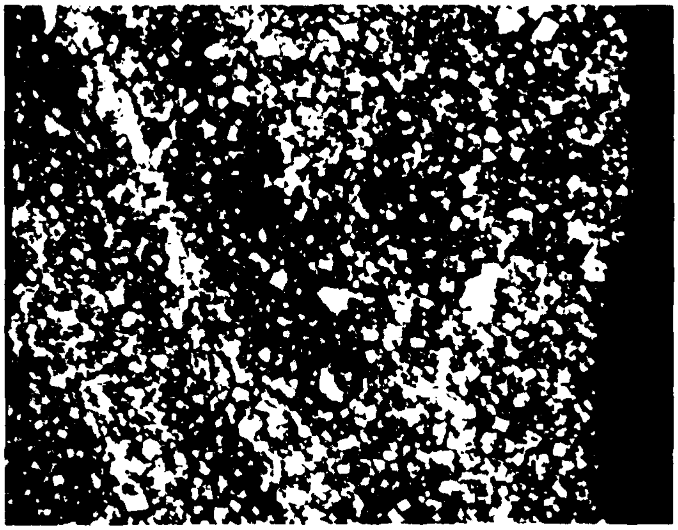

Figure 25. SEM of Lithium Surface Exposed to 0.25M $Li_2B_{10}Cl_{10}/SOCl_2$ for 8 Days at 72°C, 1000X

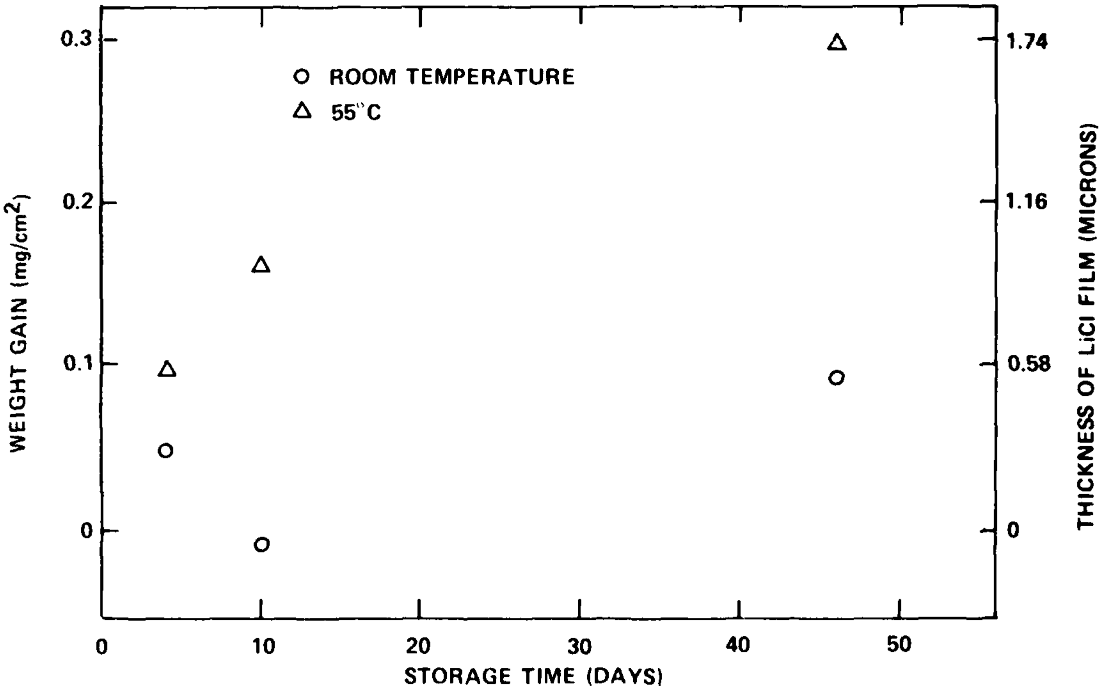

Figure 26. Weight Gain of Lithium Samples Stored in Sealed Ampoules of 0.25M $Li_2B_{10}Cl_{10}/SOCl_2$

samples stored in 0.25M $Li_2B_{10}Cl_{10}/SOCl_2$ and in 1.8M $LiAlCl_4$ at room temperature was not significant, but at 55°C the difference was appreciable, as shown in Figure 27.

The extent of film growth on lithium stored at room temperature in 0.25M $Li_2B_{10}Cl_{10}/SOCl_2$ can be compared using Figures 10, 21 and 26. After 19 days, d_{min} was about 0.035 μm; the average film thickness measured by weight gain was roughly 0.17 μm; the average size of the cubic crystals on the surface was about 1.7 μm. For storage at 55°C, the growth can be compared using Figures 11, 22 and 27. After 19 days, d_{min} was about 0.09 μm, the film thickness measured by weight gain was about 1.1 μm, and the average length of a crystal edge was approximately 8 μm.

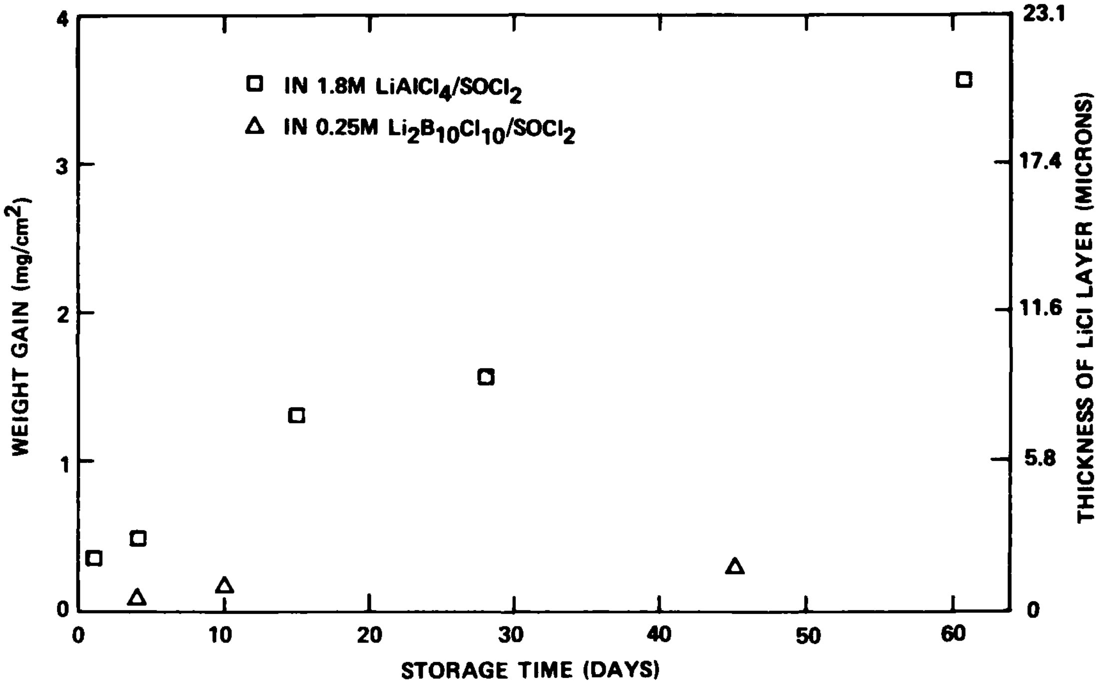

Figure 27. Weight Gain of Lithium Samples Stored at 55°C in Sealed Ampoules

3.2.4 Film Growth in 0.23M $Li_2B_{12}Cl_{12}/SOCl_2$

Weight gains for lithium samples stored in 0.23M $Li_2B_{12}Cl_{12}/SOCl_2$ as a function of time and temperature are plotted in Figure 28. The film growth rate was similar to that seen for lithium in 0.25M $Li_2B_{10}Cl_{10}$ (Figure 26). The film thickness as estimated from weight gain was about an order of magnitude larger than that calculated from capacitance measurements (Figure 14).

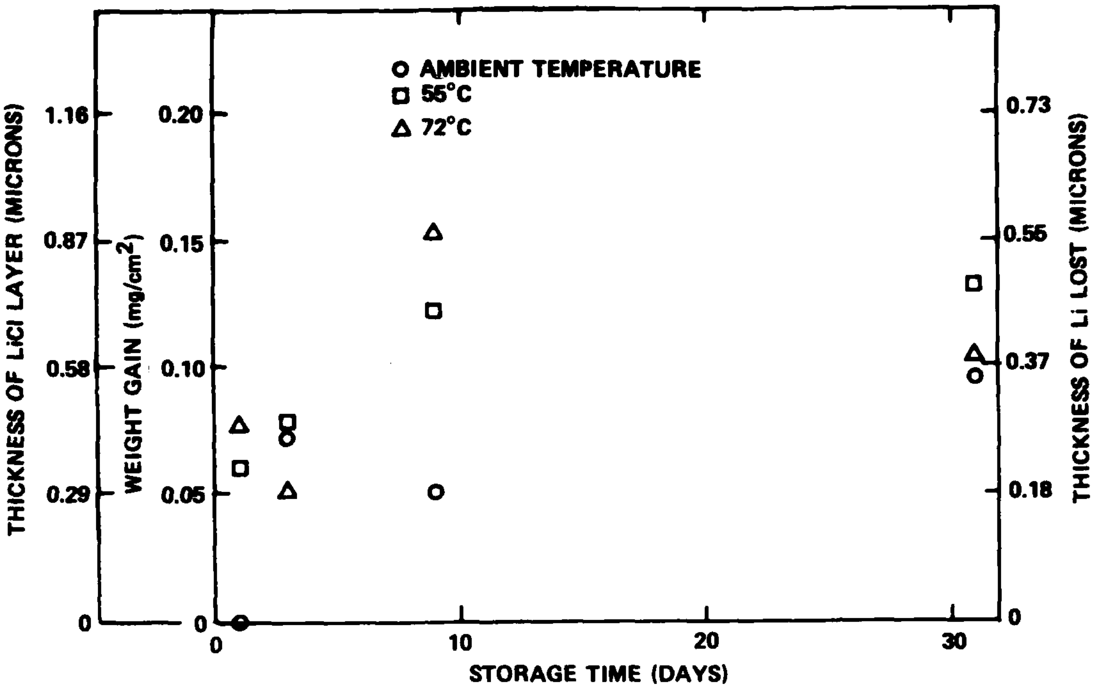

Figure 28. Weight Gain of Lithium Samples Stored in Sealed Glass Ampoules of 0.23M $Li_2B_{12}Cl_{12}/SOCl_2$

An SEM of the surface of a lithium sample stored in 0.23M $Li_2B_{12}Cl_{12}/SOCl_2$ at room temperature for 48 days is shown in Figure 29. No crystals were found. The surface appeared to have been changed from its original appearance, but was not smooth as observed in $Li_2B_{10}Cl_{10}/SOCl_2$ (Figures 21 and 23). The SEM of a surface stored for the same length of time at 55°C is shown in Figure 30. Irregularly shaped crystals with an average length of about 10 μm were found protruding from a deeper and more darkly colored (more conductive) layer of amorphous growths. An SEM of a sample stored at 72°C for 20 days is shown in Figure 31. Irregularly shaped crystals about 5 μm across were found to have grown from the surface, not visible in the photograph.

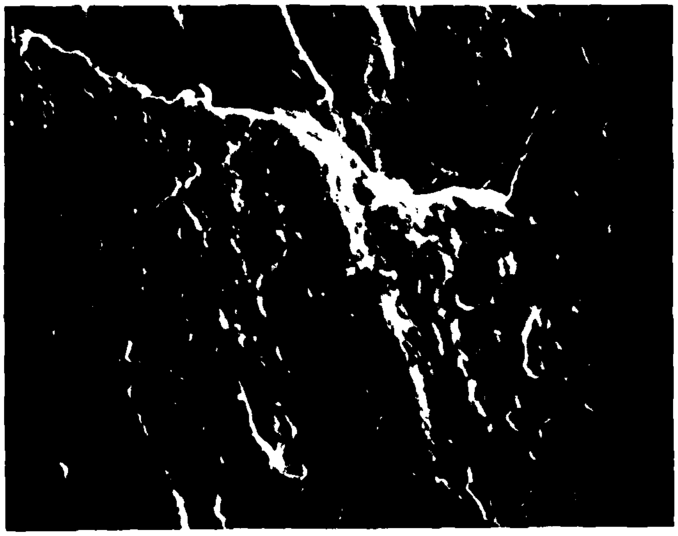

Figure 29. SEM of Lithium Surface Exposed to 0.23M $Li_2B_{12}Cl_{12}/SOCl_2$ for 48 Days at Room Temperature, 1000X at an Angle of 45° to Normal

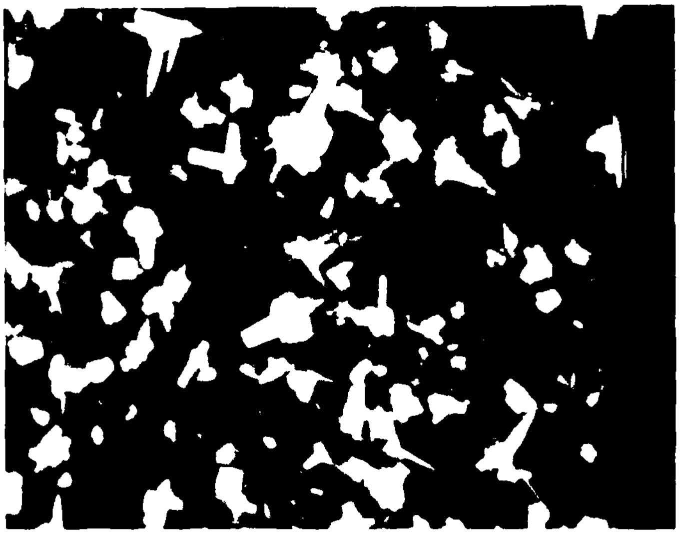

Figure 30. SEM of Lithium Surface Exposed to 0.23M $Li_2B_{12}Cl_{12}$ for 48 Days at 55°C, 1000X

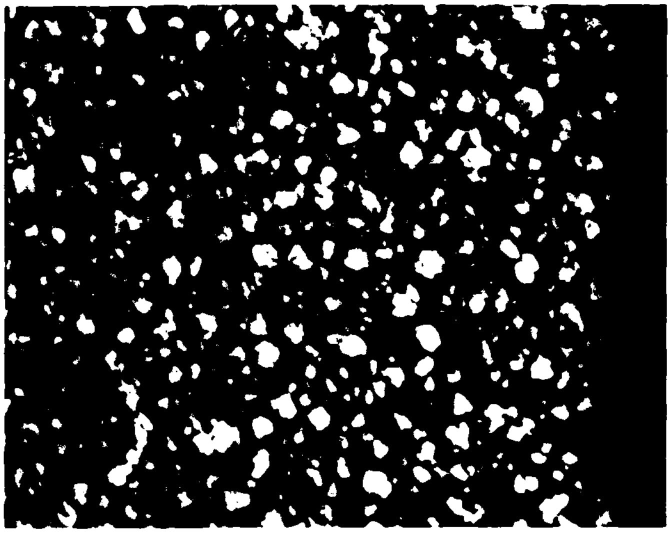

Figure 31. SEM of Lithium Surface Exposed to 0.23M $Li_2B_{12}Cl_{12}$ for 20 Days at 72°C, 1000X

3.3 VOLTAGE DELAY AND CAPACITY OF $Li/SOCl_2/C$ CELLS

3.3.1 Fresh Cells: Potential as a Function of Current Density

Polarization characteristics were determined for fresh anode limited AA cells containing 1.8M $LiAlCl_4/SOCl_2$ and 0.25M $Li_2B_{10}Cl_{10}/SOCl_2$ electrolytes at room temperature and at -20°C. A representative cell, with 1.8M $LiAlCl_4/SOCl_2$, is shown in Figure 32, and with $Li_2B_{10}Cl_{10}/SOCl_2$, in Figure 33. Cells containing $Li_2B_{10}Cl_{10}$ have been observed to operate initially at a higher potential or a first plateau (23,24). The polarization shown in Figure 33 was taken before the first plateau had been discharged. Five cells were partially discharged at various loads to remove the first plateau, then subjected to the polarization test. The results are compared in Figure 34. The first plateau allows the polarization data of fresh cells to look more optimistic than warranted.

The first plateau as it typically appears during discharge at constant load is shown in Figure 35. The charge passed during the first plateau was always less than the number of moles of $B_{10}Cl_{10}^{2-}$ contained in the electrolyte. The plateau could therefore have been caused by the kinetically favored discharge of the free radical, discussed below, resulting from the slow oxidation of $B_{10}Cl_{10}^{2-}$ by the thionyl chloride.

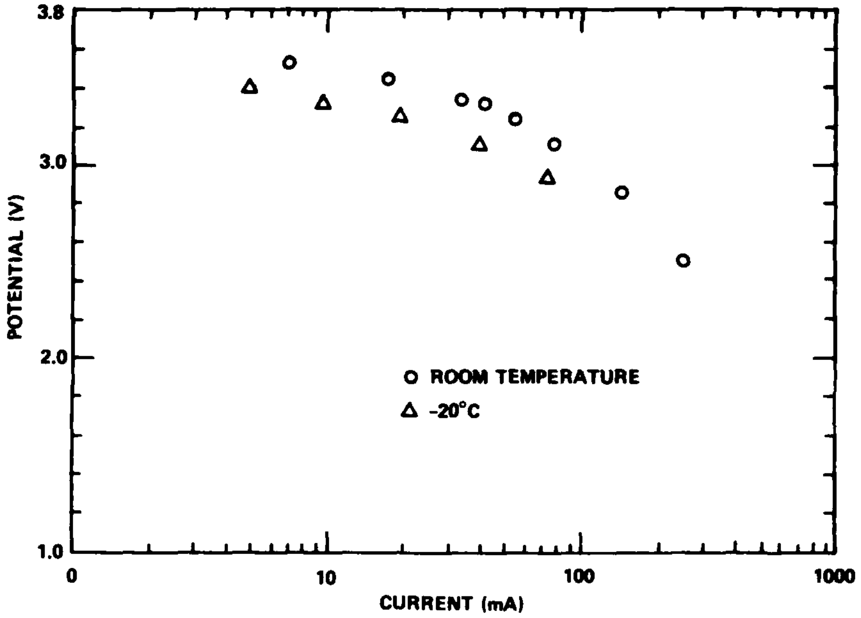

Figure 32. Polarization of AA Cells with 1.8M $LiAlCl_4/SOCl_2$ Electrolyte at Room Temperature and -20°C

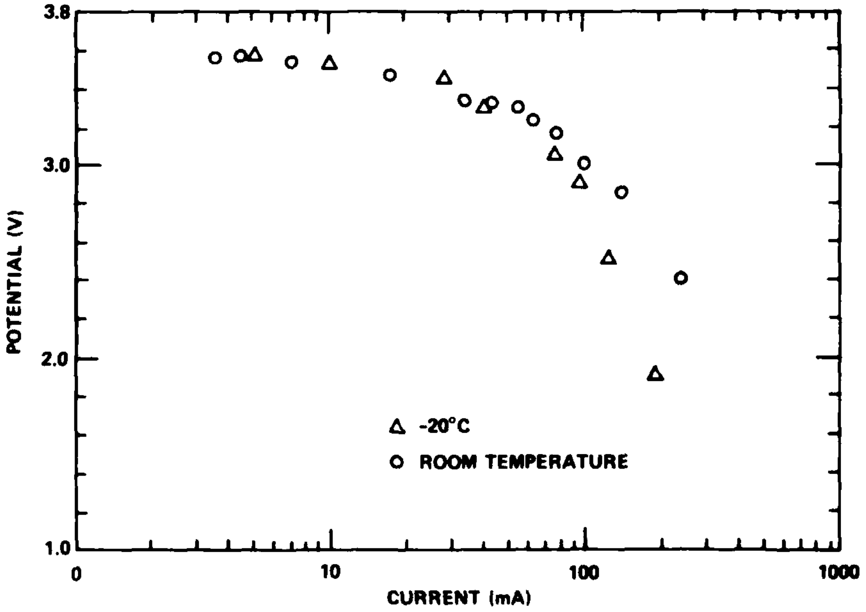

Figure 33. Polarization of AA Cells with 0.25M $Li_2B_{10}Cl_{10}/SOCl_2$ Electrolyte at Room Temperature and -20°C

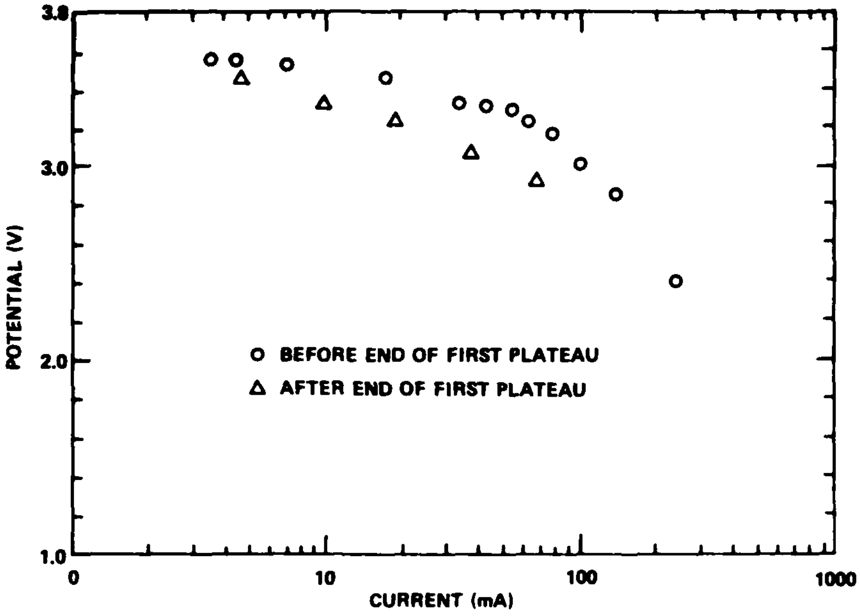

Figure 34. Polarization of AA Cells with 0.25M $Li_2B_{10}Cl_{10}/SOCl_2$ Electrolyte at Room Temperature

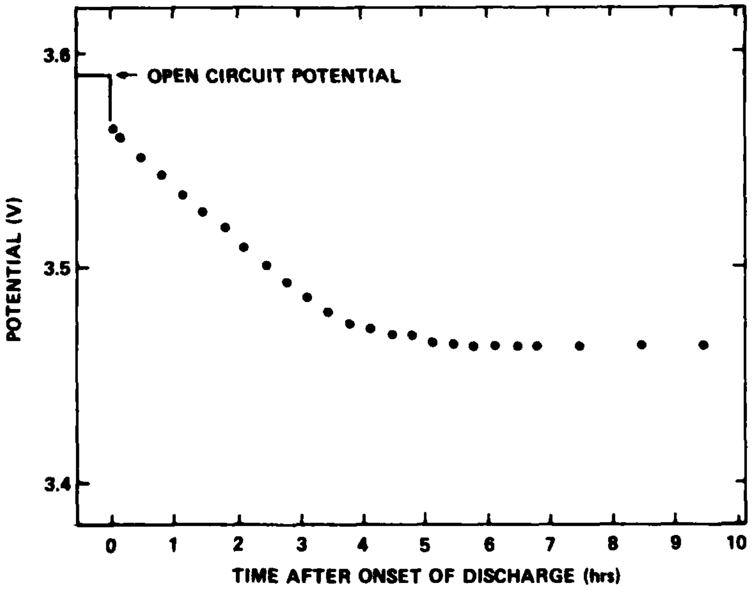

Figure 35. First Plateau Observed on Discharging AA Cell Containing 0.25M $Li_2B_{10}Cl_{10}/SOCl_2$ at a Constant Load of 750Ω at Ambient Temperature

The polarization characteristic of a representative cell containing 0.23M $Li_2B_{12}Cl_{12}/SOCl_2$ is shown in Figure 36. The room temperature polarization of cells with this electrolyte was similar to the polarization of cells with $Li_2B_{10}Cl_{10}$ after discharge of the first plateau (Figure 34). Cells with either of these electrolytes discharged at lower potential than cells with 1.8M $LiAlCl_4/SOCl_2$. The lower potential was presumably caused by lower conductivity in the polyhedral borate electrolytes relative to $LiAlCl_4/SOCl_2$, discussed below. Some of the cells containing $Li_2B_{12}Cl_{12}$ failed at -20°C when the load was reduced to 80Ω or less. Once a cell had failed it passivated and did not recover, even when the value of the load resistor was increased.

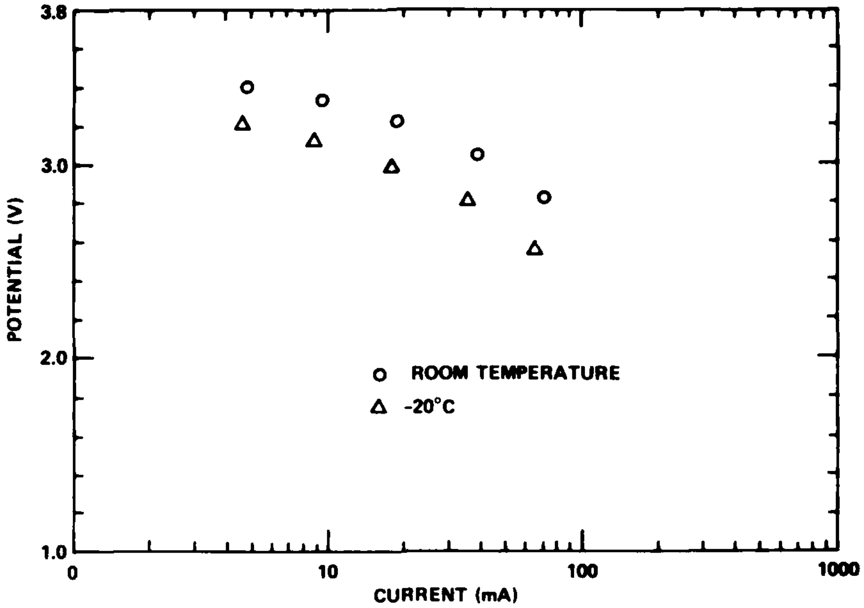

Figure 36. Polarization of AA Cells with 0.23M $Li_2B_{12}Cl_{12}/SOCl_2$ Electrolyte at Room Temperature and -20°C

3.3.2 Voltage Delay on Startup after Storage at Elevated Temperature

Following storage at 55° or 72°C for periods of two and four weeks, the AA cells were allowed to stand for at least one week at room temperature. They were then placed in a thermostated refrigerator at -20°C for three hours or more and started by connecting them to 80Ω loads. The results of the startup tests for cells containing $LiAlCl_4/SOCl_2$ after two weeks is shown in Table 4, and after four weeks in Table 5.

TABLE 4

VOLTAGE DELAY IN AA CELLS CONTAINING 1.8M $LiAlCl_4/SOCl_2$ AFTER STORAGE FOR TWO WEEKS AT ELEVATED TEMPERATURE 80Ω LOAD, -20°C

Cells Stored at 55°C (Five Duplicates)	CELL NUMBER				
	1	2	3	4	5
Seconds to minimum potential	27	40	20	30	50
Minimum potential (V)	1.8	1.6	0.45	1.6	1.4
Seconds to 2V	61	250	---	110	290
Potential at 100s (V)	2.2	1.7	0.56	1.9	1.5
Potential at 1000s (V)	2.4	2.5	1.3	(2.7)	2.6
Cells Stored at 72°C (Five Duplicates)	CELL NUMBER				
	6	7	8	9	10
Seconds to minimum potential	110	60	60	150	80
Minimum Potential (V)	1.0	1.6	1.8	1.5	1.4
Seconds to 2V	---	220	210	700	---
Potential at 100s (V)	1.0	1.7	1.8	1.8	1.4
Potential at 1000s (V)	1.6	2.6	2.4	2.2	1.6

TABLE 5

VOLTAGE DELAY IN AA CELLS CONTAINING 1.8M $LiAlCl_4/SOCl_2$ AFTER STORAGE FOR FOUR WEEKS AT ELEVATED TEMPERATURE 80Ω LOAD, -20°C

Cells Stored at 55°C (Five Duplicates)	CELL NUMBER				
	1	2	3	4	5
Seconds to minimum potential	90	60	120	70	90
Minimum potential (V)	1.0	1.2	1.2	1.0	1.2
Seconds to 2V	---	700	---	---	---
Potential at 100s (V)	1.0	1.3	1.4	1.1	1.2
Potential at 1000s (V)	1.6	2.1	1.8	1.6	1.7
Cells Stored at 72°C (Five Duplicates)	CELL NUMBER				
	6	7	8	9	10
Seconds to minimum potential	---	130	140	70	40
Minimum Potential (V)	---	2.2	1.6	1.6	1.9
Seconds to 2V	---	---	---	510	50
Potential at 100s (V)	3.0	2.2	1.6	1.6	2.2
Potential at 1000s (V)	2.8	2.6	1.8	2.2	2.4

For cells containing $Li_2B_{10}Cl_{10}/SOCl_2$, the results after two weeks are shown in Table 6, and after four weeks in Table 7. A significant portion of the cells containing 1.8M $LiAlCl_4$ failed to recover to 2V; none of the cells tested recovered to 3V in the 1000s test time (about 15 min) at -20°C. All of the cells containing 0.25M $Li_2B_{10}Cl_{10}/SOCl_2$ electrolyte recovered to 3V, and with only one exception did so in less than 25s. No cell containing this electrolyte delayed below 2V for more than 1s, although the initial discharge of these cells took place at the somewhat higher potential of the first plateau. Representative tests of voltage delay for each condition appear in Figures 37 through 44.

Voltage delay tests typical of AA cells containing 0.23M $Li_2B_{12}Cl_{12}$ after storage for two weeks at 55° and 72°C are shown in Figure 45 and 46. The results showed that these cells did not function when connected to 80Ω loads at -20°C after storage. We feel that testing of this electrolyte under less rigorous conditions is warranted.

TABLE 6

VOLTAGE DELAY IN AA CELLS CONTAINING 0.25M $Li_2B_{10}Cl_{10}/SOCl_2$
AFTER STORAGE FOR TWO WEEKS AT ELEVATED TEMPERATURE
80Ω LOAD, -20°C

Cells Stored at 55°C (Five Duplicates)	CELL NUMBER				
	1	2	3	4	5
Seconds to minimum potential	<0.5	<0.5	<0.5	<0.5	<0.5
Minimum potential (V)	2.9	2.4	2.6	2.4	2.4
Seconds to 3V	<0.5	1	<0.5	21	2
Potential at 10s (V)	3.3	3.2	3.3	2.9	3.2
Potential at 100s (V)	3.4	3.2	3.3	3.2	3.3

Cells Stored at 72°C (Three Duplicates)	CELL NUMBER		
	6	7	8
Seconds to minimum potential	<0.5	<0.5	<0.5
Minimum Potential (V)	2.8	2.8	2.9
Seconds to 3V	<0.5	8	<0.5
Potential at 10s (V)	3.2	2.0	3.2
Potential at 100s (V)	3.3	3.1	3.3

TABLE 7

VOLTAGE DELAY IN AA CELLS CONTAINING 0.25M $Li_2B_{10}Cl_{10}/SOCl_2$ AFTER STORAGE FOR FOUR WEEKS AT ELEVATED TEMPERATURE 80Ω LOAD, -20°C

Cells Stored at 55°C (Five Duplicates)	CELL NUMBER				
	1	2	3	4	5
Seconds to minimum potential	<0.5	<0.5	<0.5	<0.5	<0.5
Minimum potential (V)	2.2	2.4	1.9	2.1	1.8
Seconds to 3V	6	10	10	13	19
Potential at 10s (V)	3.1	3.0	3.0	2.9	2.8
Potential at 100s (V)	3.3	3.3	3.3	3.3	3.3
Cells Stored at 72°C (Five Duplicates)	**CELL NUMBER**				
	6	7	8	9	10
Seconds to minimum potential	<0.5	<0.5	<0.5	<0.5	<0.5
Minimum Potential (V)	2.6	2.8	2.6	2.4	3.0
Seconds to 3V	<0.5	<0.5	1	208	---
Potential at 10s (V)	3.2	3.3	3.1	2.8	3.2
Potential at 100s (V)	3.4	3.3	3.2	2.9	3.3

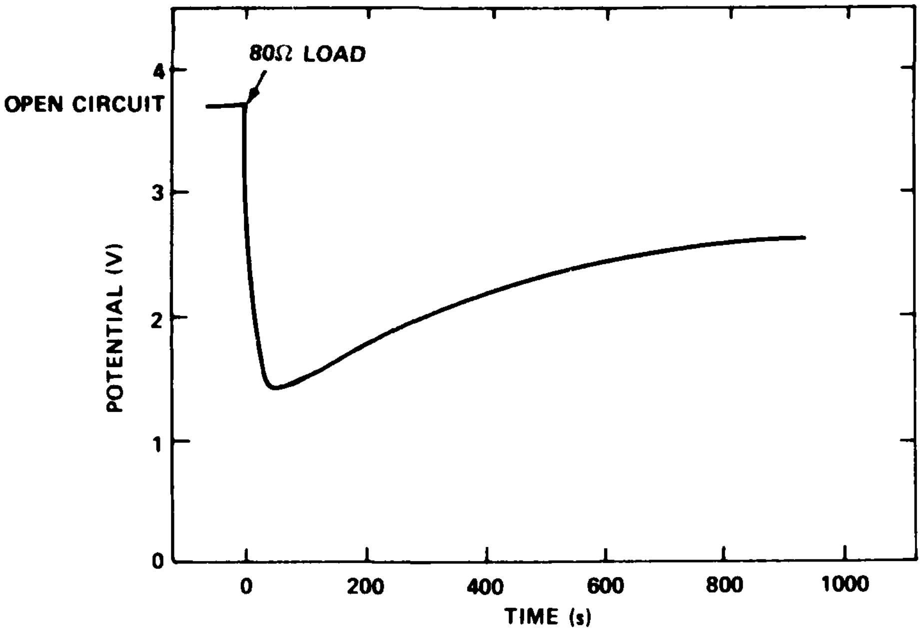

Figure 37. Representative Voltage Delay of an AA Cell at -20°C Containing $LiAlCl_4/SOCl_2$ Electrolyte after Two Weeks Storage at 55°C

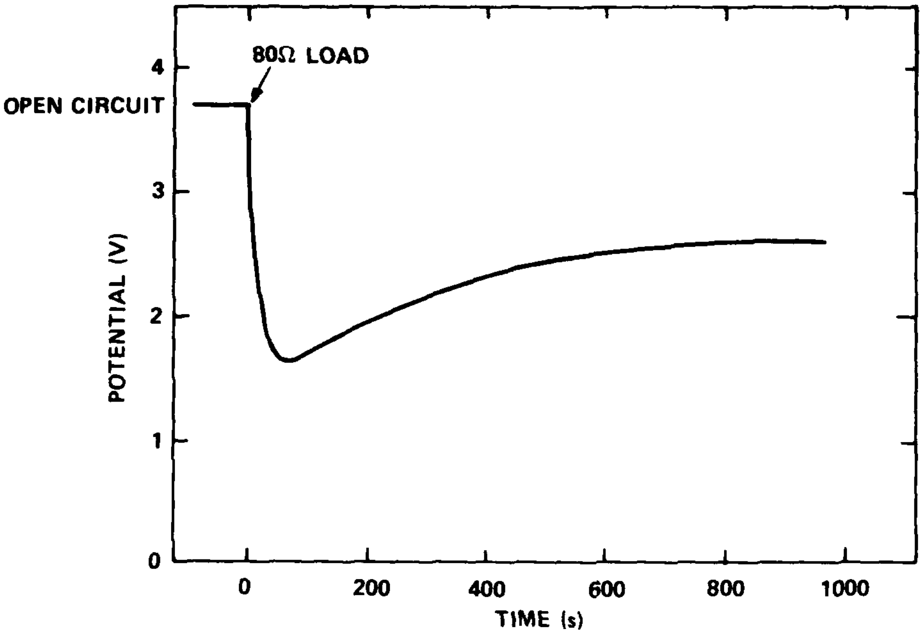

Figure 38. Representative Voltage Delay of an AA Cell at -20°C Containing 1.8M $LiAlCl_4/SOCl_2$ Electrolyte after Two Weeks Storage at 72°C

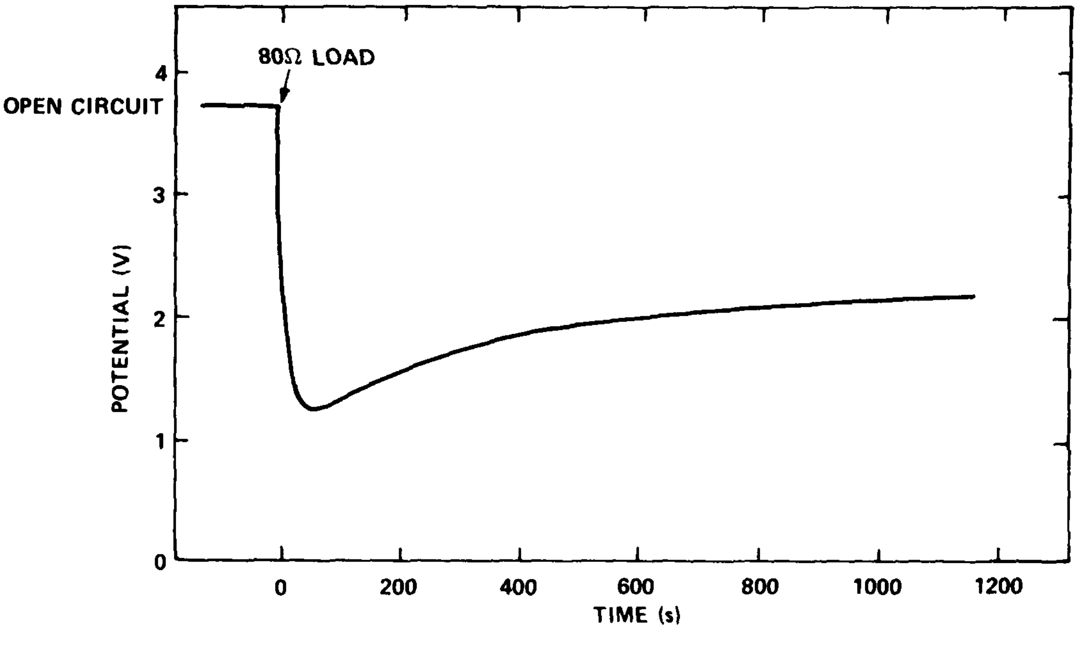

Figure 39. Representative Voltage Delay of an AA Cell at -20°C Containing 1.8M $LiAlCl_4/SOCl_2$ Electrolyte after Four Weeks Storage at 55°C

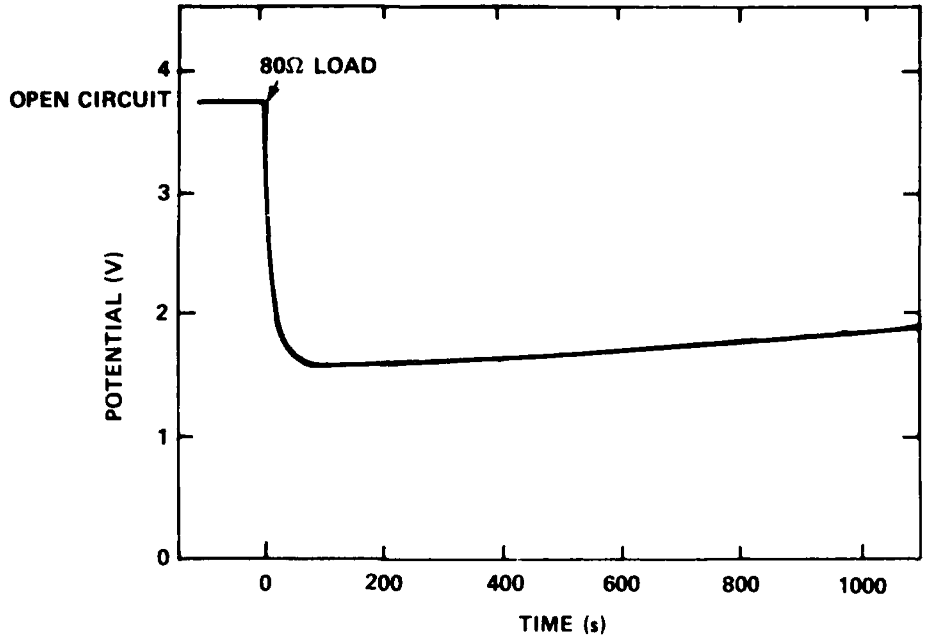

Figure 40. Representative Voltage Delay of an AA Cell at -20°C Containing 1.8M $LiAlCl_4/SOCl_2$ Electrolyte after Four Weeks Storage at 72°C

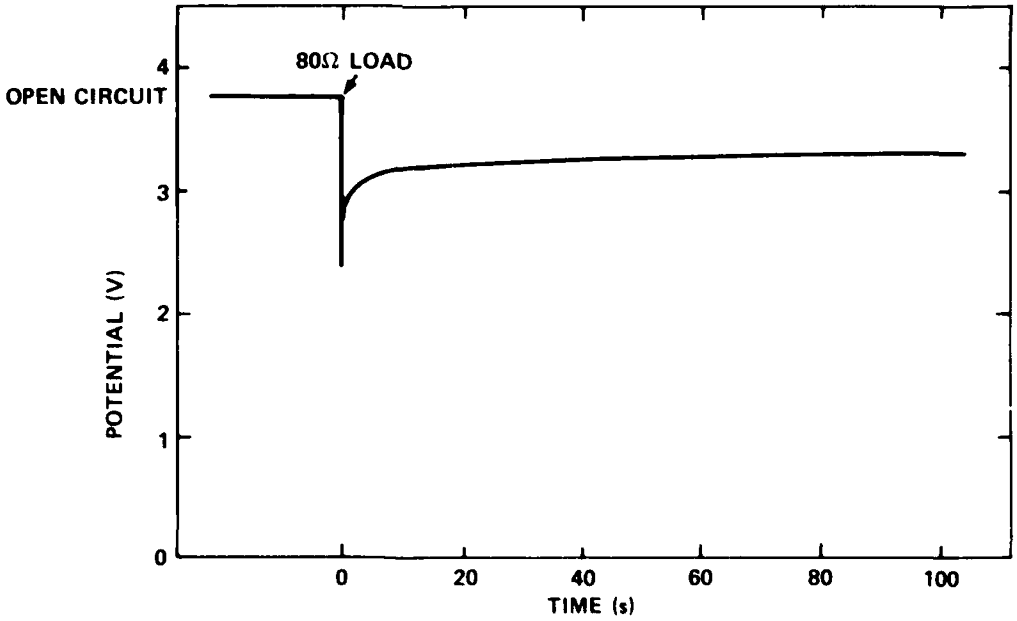

Figure 41. Representative Voltage Delay of an AA Cell at -20°C Containing 0.25M $Li_2B_{10}Cl_{10}/SOCl_2$ Electrolyte after Two Weeks Storage at 55°C

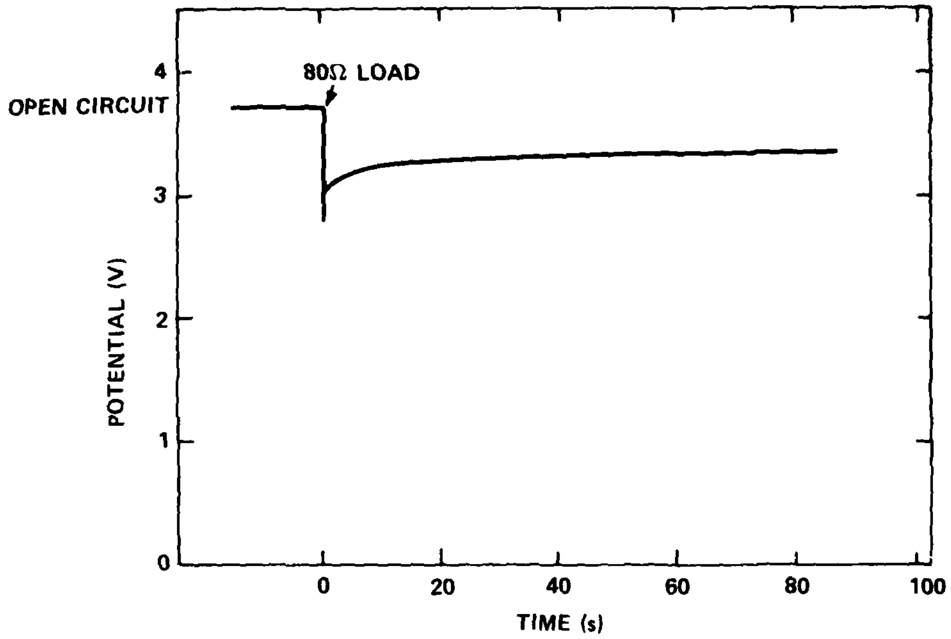

Figure 42. Representative Voltage Delay of an AA Cell at -20°C Containing 0.25M $Li_2B_{10}Cl_{10}/SOCl_2$ Electrolyte after Two Weeks Storage at 72°C

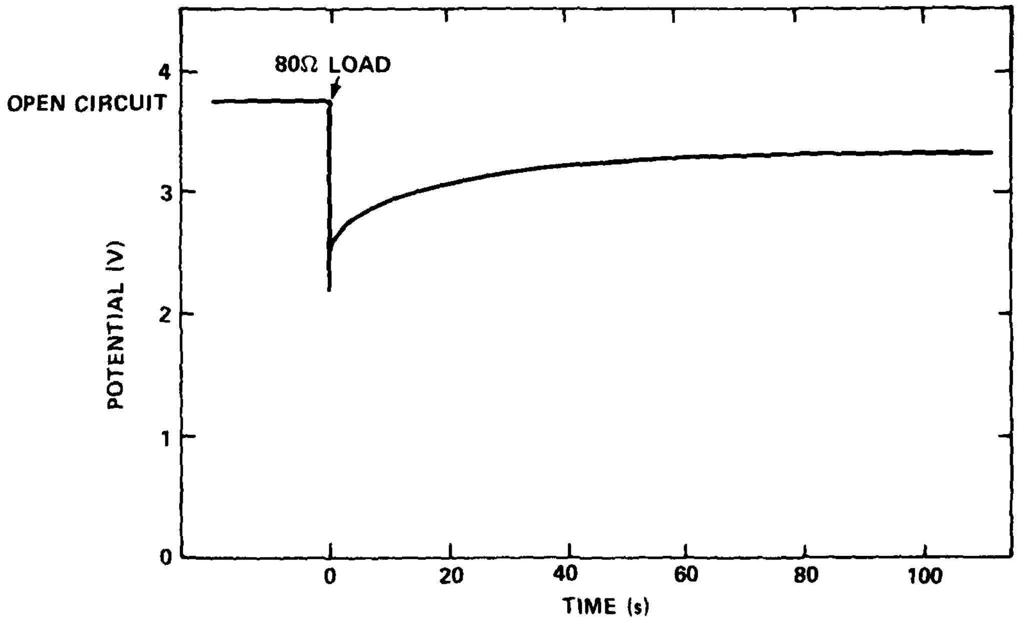

Figure 43. Representative Voltage Delay of an AA Cell at -20°C Containing 0.25M $Li_2B_{10}Cl_{10}/SOCl_2$ Electrolyte after Four Weeks Storage at 55°C

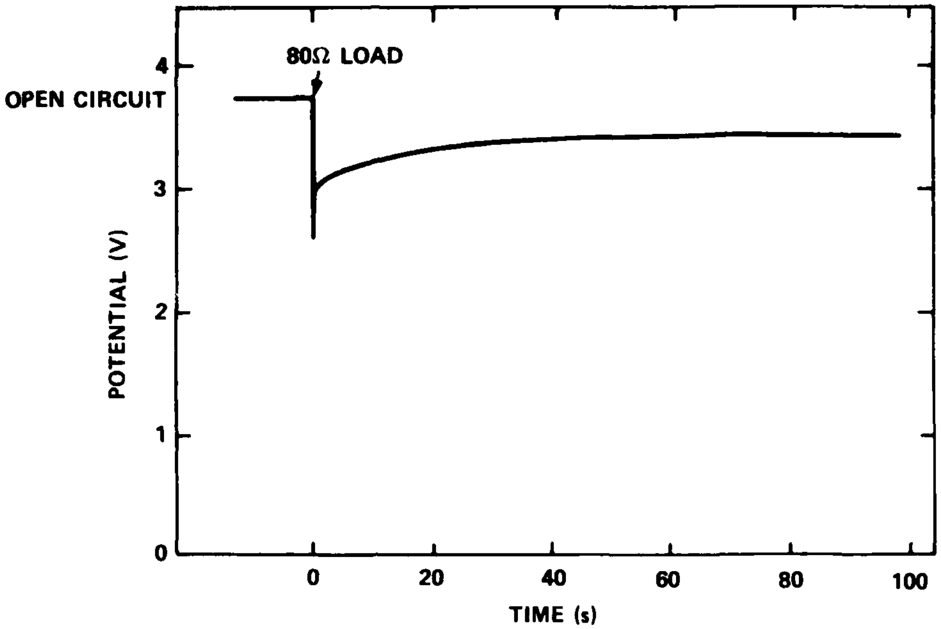

Figure 44. Representative Voltage Delay of an AA Cell at -20°C Containing 0.25M $Li_2B_{10}Cl_{10}/SOCl_2$ Electrolyte after Four Weeks Storage at 72°C

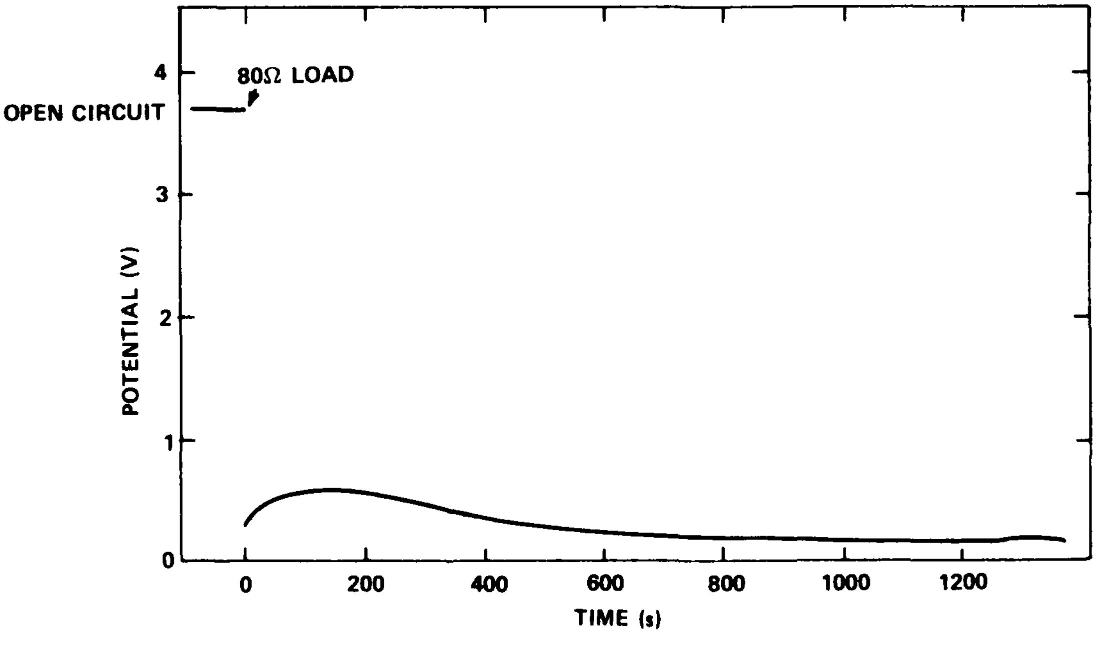

Figure 45. Voltage Delay of an AA Cell at -20°C Containing 0.23M $Li_2B_{12}Cl_{12}/SOCl_2$ Electrolyte after Two Weeks Storage at 55°C

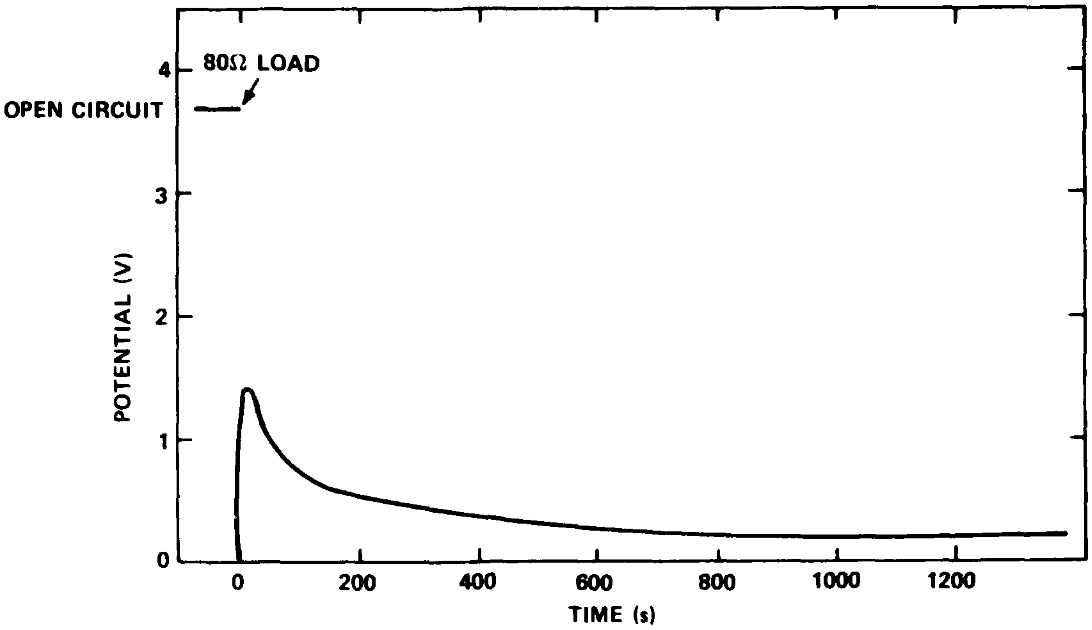

Figure 46. Voltage Delay of an AA Cell at -20°C Containing 0.23M $Li_2B_{12}Cl_{12}/SOCl_2$ Electrolyte after Two Weeks Storage at 72°C

3.3.3 Capacity Retention During Storage at Elevated Temperature

The electrical capacities of the AA size cells were measured by placing each cell on one of five different resistive loads at room temperature and monitoring the potential as a function of time. The loads used corresponded approximately to anode current densities of 6, 3, 1.5, 0.75 and 0.38 mA/cm^2. The cells were anode limited with approximately 541 mAhr of lithium in order to compare the relative effects of $LiAlCl_4$, $Li_2B_{10}Cl_{10}$ and $Li_2B_{12}Cl_{12}$ in $SOCl_2$ on lithium corrosion in $Li/SOCl_2/C$ cells during extended storage. Properly balanced AA cells using this same design have achieved better than 1.7 Ahr.

The capacities of fresh cells containing each of the three electrolytes studied in this work are shown in Table 8. Cells containing 0.23M $Li_2B_{12}Cl_{12}/SOCl_2$ gave no useful capacity when the value of the load resistor was 80Ω or less. No significant difference in the electrical capacity was found between cells with different electrolytes, although the capacities were consistently below the values expected based on the amount of lithium originally present in each cell. For all cells, the average value for the missing electrical capacity was 119 mAhr.

TABLE 8

CAPACITY OF FRESH AA CELLS DISCHARGED AT AMBIENT TEMPERATURE

Cells with 1.8M $LiAlCl_4/SOCl_2$	CELL NUMBER				
	1	2	3	4	5
Load (Ω)	43	82	172	340	750
Capacity to 2V (mAhr)	431	455	441	435	414
Capacity to 0V (mAhr)	448	455	443	435	414
Li originally present (mAhr)	561	557	555	561	555
Li lost to self-discharge (mAhr)	113	102	112	127	141
Average capacity missing: 119 mAhr (std. dev. = 12.7%)					

Cells with 0.25M $Li_2B_{10}Cl_{10}/SOCl_2$	CELL NUMBER				
	6	7	8	9	10
Load (Ω)	43	82	172	340	750
Capacity to 2V (mAhr)	401	439	444	450	425
Capacity to 0V (mAhr)	431	442	452	470	425
Li originally present (mAhr)	554	551	559	555	559
Li lost to self-discharge (mAhr)	123	109	107	85	134
Average capacity missing: 112 mAhr (std. dev. = 16.6%)					

Cells with 0.23M $Li_2B_{12}Cl_{12}/SOCl_2$	CELL NUMBER				
	11	12	13	14	15
Load (Ω)	43	82	172	340	750
Capacity to 2V (mAhr)	---	---	401	351	297
Capacity to 0V (mAhr)	424	414	446	460	409
Li originally present (mAhr)	560	554	557	556	560
Li lost to self-discharge (mAhr)	136	140	111	96	151
Average capacity missing: 127 mAhr (std. dev. = 17.8%)					

The loss of capacity observed for these fresh cells could have been caused by direct reaction of lithium with thionyl chloride or by electrochemical oxidation of the lithium at the expense of thionyl chloride reduced on cell hardware in electrical contact with the lithium. The direct chemical reaction would have been moderated by the formation of lithium chloride on the surface, but could have been aggravated through disruption of the lithium chloride film during electrochemical oxidation of the lithium. From the information obtained in this report, estimations of the amount of lithium lost through direct chemical reaction, assuming that film disruption by electrochemical oxidation does not significantly aggravate corrosion, can be estimated. From Figure 18, the film thickness calculated from the weight gain of a lithium sample stored at room temperature in 1.8M $LiAlCl_4/SOCl_2$ was about 2.4 μm after ten days, corresponding to 4 mAhr over an area of 13 cm^2. From Figure 26, a lithium sample stored at room temperature for ten days in 0.25M $Li_2B_{10}Cl_{10}$ acquired a layer about 0.2 μm thick, or 0.3 mAhr over an area of 13 cm^2. Estimation of lithium consumed by local cell reaction was previously measured at 72°C (3,17).

Capacities of AA cells containing $LiAlCl_4$ and $Li_2B_{10}Cl_{10}$ electrolytes after storage for two and four weeks at 55° or 72°C are shown in Tables 9 through 12.

TABLE 9

CAPACITY OF AA CELLS CONTAINING $LiAlCl_4/SOCl_2$ AFTER TWO WEEKS AT ELEVATED TEMPERATURE, DISCHARGED AT AMBIENT TEMPERATURE

Cells Stored at 55°C	CELL NUMBER				
	1	2	3	4	5
Load (Ω)	43	82	172	340	750
Capacity to 2V (mAhr)	329	325	353	360	329
Capacity to 0V (mAhr)	351	335	369	361	329
Li originally present (mAhr)	559	562	561	558	555
Li lost to self-discharge (mAhr)	208	227	192	197	226
Average capacity missing: 210 mAhr (std. dev. = 7.7%)					

Cells Stored at 72°C	CELL NUMBER			
	6	7	8	9
Load (Ω)	43	82	172	340
Capacity to 2V (mAhr)	247	293	316	327
Capacity to 0V (mAhr)	324	388	328	329
Li originally present (mAhr)	555	559	559	553
Li lost to self-discharge (mAhr)	231	171	231	224
Average capacity missing: 214 mAhr (std. dev. = 13.5%)				

TABLE 10

CAPACITY OF AA CELLS CONTAINING 1.8M $LiAlCl_4/SOCl_2$ AFTER FOUR WEEKS AT ELEVATED TEMPERATURE, DISCHARGED AT AMBIENT TEMPERATURE

Cells Stored at 55°C	CELL NUMBER				
	1	2	3	4	5
Load (Ω)	43	82	172	340	750
Capacity to 2V (mAhr)	263	302	336	350	283
Capacity to 0V (mAhr)	359	337	339	353	283
Li originally present (mAhr)	555	560	561	557	562
Li lost to self-discharge (mAhr)	196	223	222	206	279
Average capacity missing: 225 mAhr (std. dev. = 14.3%)					

Cells Stored at 72°C	CELL NUMBER				
	6	7	8	9	10
Load (Ω)	43	82	172	340	750
Capacity to 2V (mAhr)	198	298	320	325	310
Capacity to 0V (mAhr)	279	313	331	328	319
Li originally present (mAhr)	559	559	558	560	550
Li lost to self-discharge (mAhr)	280	246	227	232	231
Average capacity missing: 243 mAhr (std. dev. = 9.0%)					

TABLE 11

CAPACITY OF AA CELLS CONTAINING 0.25M $Li_2B_{10}Cl_{10}/SOCl_2$ AFTER TWO WEEKS AT ELEVATED TEMPERATURE, DISCHARGED AT AMBIENT TEMPERATURE

Cells Stored at 55°C	CELL NUMBER				
	1	2	3	4	5
Load (Ω)	82	172	172	340	750
Capacity to 2V (mAhr)	368	409	399	403	385
Capacity to 0V (mAhr)	392	413	408	405	397
Li originally present (mAhr)	555	557	556	558	557
Li lost to self-discharge (mAhr)	164	144	148	153	160
Average capacity missing: 154 mAhr (std. dev. = 5.4%)					

Cells Stored at 72°C	CELL NUMBER	
	6	7
Load (Ω)	43	750
Capacity to 2V (mAhr)	295	415
Capacity to 0V (mAhr)	386	416
Li originally present (mAhr)	553	561
Li lost to self-discharge (mAhr)	167	145
Average capacity missing: 156 mAhr		

TABLE 12

CAPACITY OF AA CELLS CONTAINING 0.25M $Li_2B_{10}Cl_{10}/SOCl_2$ AFTER
FOUR WEEKS AT ELEVATED TEMPERATURE, DISCHARGED
AT AMBIENT TEMPERATURE

Cells Stored at 55°C	CELL NUMBER				
	1	2	3	4	5
Load (Ω)	43	82	172	340	750
Capacity to 2V (mAhr)	324	365	344	423	459
Capacity to 0V (mAhr)	351	401	375	424	459
Li originally present (mAhr)	560	560	560	560	560
Li lost to self-discharge (mAhr)	208	158	183	135	100
Average capacity missing: 157 mAhr (std. dev. = 26.7%)					

Cells Stored at 72°C	CELL NUMBER		
	6	7	8
Load (Ω)	43	172	750
Capacity to 2V (mAhr)	318	257	367
Capacity to 0V (mAhr)	376	271	371
Li originally present (mAhr)	554	554	561
Li lost to self-discharge (mAhr)	175	283	190
Average capacity missing: 216 mAhr (std. dev. = 27%)			

The maximum amount of lithium which could have been consumed by direct reaction, that is, after storage at 72°C for one month in 1.8M $LiAlCl_4$, was shown in Figure 18. About 17 μm of lithium would be corroded corresponding to only about 30 mAhr for a 13-cm^2 anode. The amount of lithium found missing was clearly in excess of this value for all of the measurements made, although corrosion likely contributed to the total loss. Local discharge against cell hardware, measured by holding stainless steel samples at the lithium potential with a potentiostat, was reported to be 110 mAhr/cm^2 during storage at 72°C for four weeks, with 25% of the total consumption occurring during the first 2.5 hrs (3,17). The cells used for the present tests are estimated to have an area of 1 to 2 cm^2 of stainless steel in electrical contact with both the lithium and the electrolyte. The amount of lithium consumed at 72°C for one month by coating the stainless steel exposed, plus that consumed during film formation on Li, is therefore estimated to be between 130 and 240 mAhr for a 13-cm^2 anode AA cell. In the case of $Li_2B_{10}C_{10}$, as compared with $LiAlCl_4$, the results after storage at 72°C suggest that not only is less lithium consumed in coating the lithium surface, but less is consumed in coating the cell hardware with lithium chloride.

3.4 PHYSICAL CHEMICAL PROPERTIES OF $Li_2B_{10}Cl_{10}/SOCl_2$ AND $Li_2B_{12}Cl_{12}/SOCl_2$

3.4.1 Conductivity as a Function of Temperature and Time

The conductivities of $Li_2B_{10}Cl_{10}$ and $Li_2B_{12}Cl_{12}$ were measured as a function of temperature at 0.1N,* and 0.25N; and the conductivities of $Li_2B_{10}Cl_{10}$ and $LiAlCl_4$ were measured as a function of temperature at 0.5N. The results are plotted in Figures 47 and 48. The conductivities of solutions of $Li_2B_{10}Cl_{10}$ were taken several hours after preparation, and were not reproducible between the cooling and warming cycles except at the highest concentration. Measurements for $Li_2B_{12}Cl_{12}$ and $LiAlCl_4$ were reproducible. Figure 49 shows log conductivity vs. the reciprocal of the absolute temperature for "fresh" 0.1N and 0.25N $Li_2B_{10}Cl_{10}$ compared with "aged" solutions, the 0.1N solution having been remeasured after 19 days and the 0.25N solution after nine days. Both were not reproducible between the cooling and the warming cycles, but the conductivities were from 30% to 80% higher than they had been.

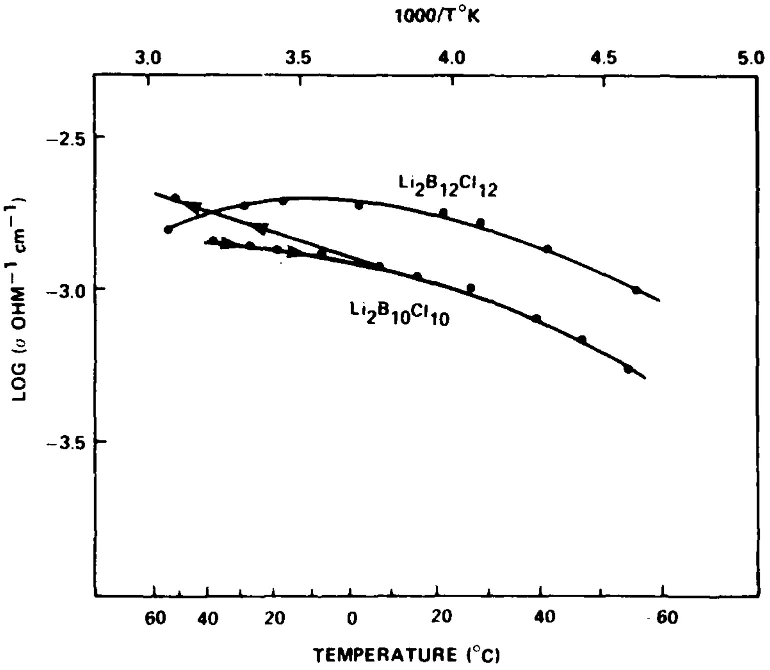

Figure 47. Log σ vs. 1000/T for 0.25N $Li_2B_{10}Cl_{10}$ and $Li_2B_{12}Cl_{12}$ in $SOCl_2$

---

*N = Equivalents per liter.

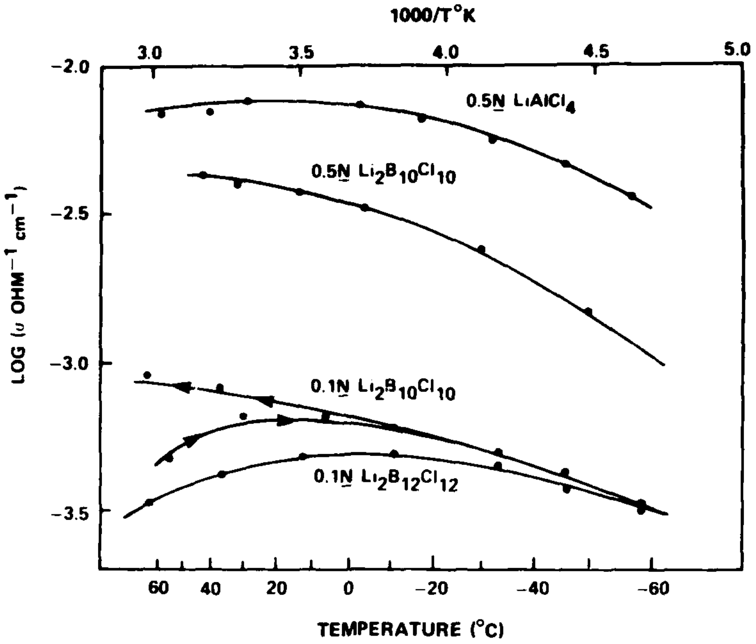

Figure 48. Log σ vs. 1000/T for 0.1N $Li_2B_{10}Cl_{10}$ and $Li_2B_{12}Cl_{12}$, and 0.5N $Li_2B_{10}Cl_{10}$ and $LiAlCl_4$, in $SOCl_2$

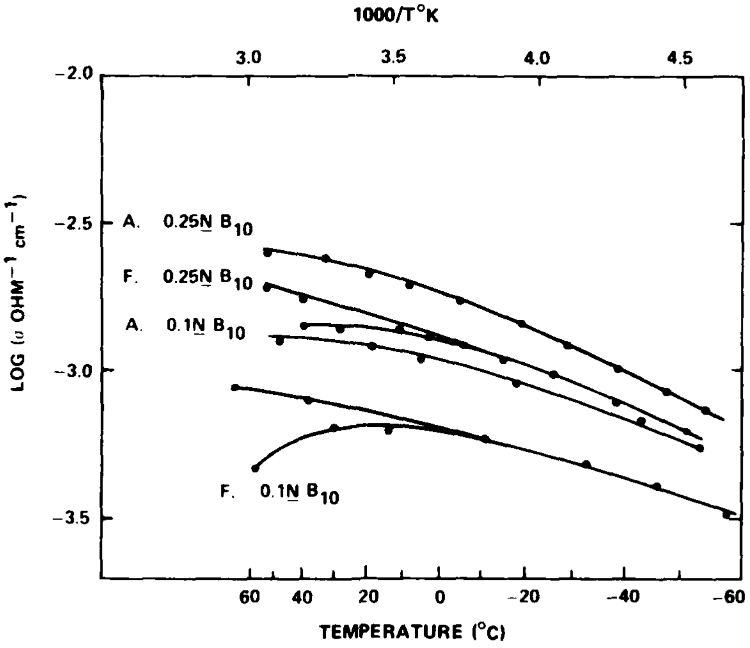

Figure 49. Log σ vs. 1000/T for 0.1N and 0.25N $Li_2B_{10}Cl_{10}$ in $SOCl_2$ before (Fresh) and after (Aged) Storage at Room Temperature

Solutions containing $Li_2B_{10}Cl_{10}$ were found to have formed white crystalline precipitates during aging, which were identified as pure lithium chloride. The supernatant solutions contained the same concentration of $B_{10}Cl_{10}^{2-}$, measured gravimetrically using aqueous tetraphenylarsonium chloride or triphenylmethylphosphonium bromide and hydrolyzed aliquots from the electrolyte solutions. Infrared spectra showed that the anions had not been altered. White crystals of LiCl also formed in flasks containing $SOCl_2$ solutions of $Li_2B_{12}Cl_{12}$, but the rate of reaction was far slower, taking several months rather than several days.

The conductivity of these solutions is likely affected by the degree of dissociation and the ionic mobility of the resulting ions. Lithium tetracholoroaluminate may be more conductive at 0.5N than is $Li_2B_{10}Cl_{10}$ because the mobility of $AlCl_4^-$ is higher than $B_{10}Cl_{10}^{2-}$ due to its smaller size and its smaller charge. The univalent anion might allow greater ionic dissociation of $LiAlCl_4$ relative to $Li_2B_{10}Cl_{10}$. The increase in conductivity and the simultaneous precipitation of LiCl noted on aging $Li_2B_{10}Cl_{10}/SOCl_2$ solutions could have resulted from the gradual formation of a uninegative anion produced during the oxidation of $B_{10}Cl_{10}^{2-}$ by $SOCl_2$:

$$SOCl_2 + Li^+ + B_{10}Cl_{10}^{2-} \rightarrow SOCl\cdot + B_{10}Cl_{10}^{-}\cdot + \underline{LiCl}$$

The presence of at least one stable free radical $SOCl_2$ solutions of $Li_2B_{10}Cl_{10}$ is discussed below in Section 3.4.3.

3.4.2 Thermal Stability of $Li_2B_{10}Cl_{10}$ and $Li_2B_{12}Cl_{12}$

Both $Li_2B_{10}Cl_{10}$ were found to have limited thermal stability. A sample of $Li_2B_{10}Cl_{10}$ when heated to 200°C in vacuum discolored slightly but noticeably. When heated to 300°C overnight it discolored extensively. When a sample of this material was taken for testing not all of it dissolved in water, some of it reacted with water, and free chloride was detected when silver nitrate was added to the acidified solution. This shows that the $Li_2B_{10}Cl_{10}$ was at least partially decomposed on heating to 300°C. A sample of $Li_2B_{12}Cl_{12}$ turned light gray when heated to 300°C.

The thermal stability of other $B_{10}Cl_{10}^{2-}$ derivatives has been previously discussed (26). $Cs_2B_{10}Cl_{10}$ suffered only 4% weight loss when heated <u>in vacuo</u> to 600°C. In contrast, $H_2B_{10}Cl_{10}\cdot 4\ H_2O$ decomposed completely when heated to 260°C <u>in vacuo</u> for 5 hrs (27). We assumed that $B_{10}Cl_{10}^{2-}$ was unstable in the latter case because of reactions involving aqueous acid. This assumption appears to be oversimplified.

Our results suggest that the size of the action affects the stability of the anion. The larger the cation, the more stable is the anion. Cation size has been observed to affect the stability of BX_4^- salts where X is a halogen. BCl_4^- salts, for example, are less stable with small cations (28,29). On the basis of x-ray structures for $B_{10}H_{10}^{2-}$ (30) and $B_{12}H_{12}^{2-}$ (31) and covalent and van der Walls radii (32), the chlorine atoms in both $B_{10}Cl_{10}^{2-}$ and $B_{12}Cl_{12}^{2-}$ are almost touching. Polarizing cations such as lithium are apparently able at high temperature to abstract chloride from the anionic moiety.

The thermal stability of these anions, therefore, appears to be affected by two parameters. One is the chloride-chloride repulsion, a steric effect, which can lower the strength of the molecular bonding. The other is the ability of a cation which high charge density, such as Li^+, to polarize the anion and in this case remove the chloride to form LiCl, which has a much higher lattice stabilization energy than the lithium salt of the polyhedral borate.

It has been necessary to heat these salts for prolonged periods of time at reduced pressure in order to remove solvents following the final recrystallization in the purification after synthesis. If the temperature is increased to reduce the time required, partial or total decomposition of the salts is now known to result.

3.4.3 Visible and EPR Spectra of $Li_2B_{10}Cl_{10}/SOCl_2$

A visible spectrum of a dilute solution of $Li_2B_{10}Cl_{10}$ in $SOCl_2$ produced the result shown in Figure 50. While solutions of $Li_2B_{10}Cl_{10}$ in $SOCl_2$ appeared violet (20,22), both the salt and the solvent were colorless prior to the preparation of the solutions. Two absorptions were found, a prominent peak at 57.5 nm and another less prominent one at 52.5 nm. The spectrum shown in Figure 50 was taken shortly after mixing.The spectrum became more intense over a period of four days and then did not change any further. The formation of complexes and solvolysis reactions have been suggested to explain the color of these solutions, and the solid lithium chloride which crystallized on standing (22).

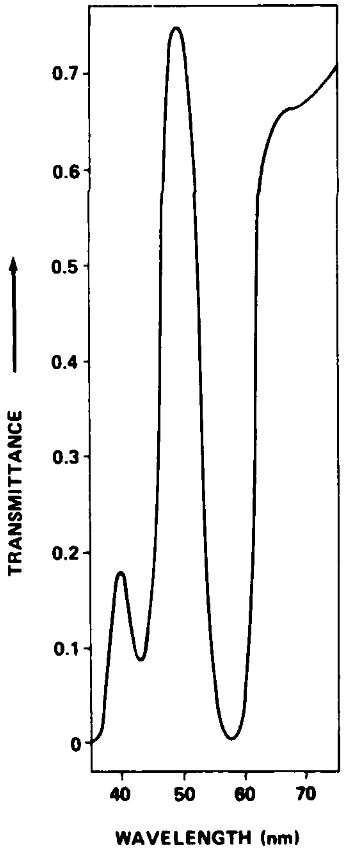

Figure 50. Visible Spectrum of $Li_2B_{10}Cl_{10}/SOCl_2$

The aqueous and nonaqueous oxidation of $B_{10}H_{10}^{2-}$ to a free radical with an absorption centered at about 55.0 nm has been reported (33-35). The final products of the oxidation that forms the blue solution containing this free radical appear to be partially halogenated polyhedral borates of the formula $B_{10}Cl_{x}B_{10-x}^{2-}$ (35). The anions $B_{10}H_{10}^{2-}$ and $B_{12}H_{12}^{2-}$ also have been electrochemically oxidized, $B_{10}H_{10}^{2-}$ reversibly forming a free radical on oxidation (36). The anion $B_{10}H_{10}^{2-}$ is a precursor of $B_{10}Cl_{10}^{2-}$ and has a similar configuration and electronic structure.

On the basis of the literature already cited, the violet color in $Li_2B_{10}Cl_{10}/SOCl_2$ might have been caused by the oxidation of the borate by thionyl chloride to produce a free radical. An electron paramagnetic resonance signal was indeed observed to develop over a period of four days following the dissolution of $Li_2B_{10}Cl_{10}$ in $SOCl_2$. The signal increased in the same time frame that the visible spectrum was observed to increase. The EPR g factor, or gyromagnetic ratio, was about two, which is typical of many free radiacals. The peak-to-peak width of the signal was about 640G, which is unusually broad. Since boron is about 20% B_{10} and 80% B_{11} and there are ten atoms in each polyhedral borate moiety, the number of lines expected from hyperfine splitting would be very large. No hyperfine splittings were observed. The free radical may be in a molecular orbital with about 20% to 30% atomic S orbital involvement. The strength of the signal indicated that it did not arise from an impurity or a minor reaction product.

The EPR signal was unaffected by whether the solution of $Li_2B_{10}Cl_{10}$ in $SOCl_2$ were made in air or vacuum or whether lithium was present. Upon evaporation, a signal was observed in the dark solid residue left behind. A sample of such residue, when hydrolized, was observed to give a violet color which persisted in solution for some hours. It was previously reported that $B_{10}Cl_{10}^{2-}$ can be recovered unchanged upon hydrolysis of $Li_2B_{10}Cl_{10}$ $SOCl_2$ (22). The resulting aqueous solution was colorless, but this could have resulted from the reduction of the radical in aqueous solution by the sulfur dioxide present as the product of hydrolysis of $SOCl_2$.

The violet color and the radical formation by $Li_2B_{10}Cl_{10}$ in $SOCl_2$ may be associated with the presence of the strongly polarizing lithium cation. For example, the bis-triethylammonium salt of $B_{10}Cl_{10}^{2-}$ when dissolved in $SOCl_2$ did not produce a violet colored solution (22). Similarly, the electrochemical oxidation of $B_{10}H_{10}^{2-}$ and its derivatives has been found to be affected by the cation present in solution. The potential of polarographic oxidation of $B_{10}H_8(OH)_2^{2-}$ in aqueous solution was dependent upon the composition of the buffer solution used to vary the pH (37). These authors noted the inconsistency in their results but offered no explanation. The oxidation potential of $B_{10}H_{10}^{2-}$ in acetonitrile was reported to be +0.375V vs. a standard calomel electrode in 0.1M $LiClO_4$, but +0.43V in 0.1M tetraethylammonium perchlorate (36).

The formation and persistence of a free radical in $Li_2B_{10}Cl_{10}/SOCl_2$ may be related to the "noncrystallographic" nature of the smooth passivating layer observed on lithium as described above, and ultimately to the mechanism by which $Li_2B_{10}Cl_{10}$ moderates the voltage delay problem. Solutions of lithium tetrachloroaluminate may differ from $Li_2B_{10}Cl_{10}/SOCl_2$ in having no stable free radical present in solution. The intermediate formed on discharge of $Li/SOCl_2$ cells could be a free radical such as $\cdot SO \cdot$ or $SOCl_2 \cdot$, but the intermediate decomposes slowly even at ambient temperature to sulfur and sulfur dioxide (39). In the studies described in this report, the only discharge products present in solution were those present as the result of the direct reduction of the solvent by lithium metal. Dey has noted that $B_{10}Cl_{10}^{2-}$ reduces the delay relative to an electrolyte containing only $AlCl_4^-$ when both anions are present at the same time (25). The anion $B_{10}Cl_{10}^{2-}$ evidently plays an active role in reducing the delay and is not just a passive substitute for $AlCl_4^-$. Introduction of materials capable of producing stable free radicals in $LiAlCl_4/SOCl_2$ may aid in reducing electrochemical passivation and voltage delay in $Li/SOCl_2$ cells.

4. CONCLUSIONS AND RECOMMENDATIONS

4.1 TASK I - INVESTIGATION OF ANODE-SOLUTE INTERACTIONS

The monitoring of the film growth rate on lithium by pulse polarization techniques has shown that the electrical capacitance per unit area of lithium was higher when stored with $Li_2B_{10}Cl_{10}$ $SOCl_2$ than it was when stored with $LiAlCl_4$ $SOCl_2$, and that the resistance per unit area was substantially lower as a function of time. At higher temperature the capacitance was lower and the resistance higher. According to the solid electrolyte interphase model, chemically passivating salt films which formed on lithium in the polyhedral borate electrolyte were considerably thinner and more conductive. As the storage temperature was increased, the growth rate of the film was higher for both electrolytes.

The film growth rate, when measured by the gain in weight of lithium samples stored in $SOCl_2$ or electrolyte as a function of time, also indicated that salt films which formed in $Li_2B_{10}Cl_{10}$ $SOCl_2$ are much thinner than in $LiAlCl_4$ $SOCl_2$. When compared with film thicknesses measured by the pulse polarization technique, the thicknesses measured by weight gain are larger on lithium in $Li_2B_{10}Cl_{10}$ $SOCl_2$, just as previously reported for lithium in $LiAlCl_4$ $SOCl_2$. In parallel with the results obtained previously and during the course of this work, the chemically passivating layer appears to consist of a thin impervious region nearest the metal, covered by a porous or irregularly shaped overlayer. As the storage temperature was increased, the rate of film growth as measured by weight gain also increased, whether the electrolyte was $LiAlCl_4$ $SOCl_2$ or $Li_2B_{10}Cl_{10}$ $SOCl_2$.

Lithium samples which had been stored with electrolyte in glass ampoules were found during examination under the scanning electron microscope to have acquired layers of corrosion products whose appearance was dependent on the composition of the solution. When stored in $LiAlCl_4$ $SOCl_2$, a closely packed crystalline layer was found showing chloride by EDAX, but no aluminum or sulfur. The photographs were similar to ones obtained during previous investigations. The crystals were larger for higher storage temperature or longer storage time. When only $SOCl_2$ was used, lithium acquired a crystalline surface only during storage at elevated temperature. The surface showed chlorine by EDAC except in occasional irregularities, which contained both S and Cl. When $Li_2B_{10}Cl_{10}$ $SOCl_2$ was used, the surface acquired a smooth layer, much smoother than the original lithium, showing chloride but no sulfur. The unique chemically passivating layer caused by the boron salt is likely the reason why $B_{10}Cl_{10}^{=}$ alleviates the delay problem in Li $SOCl_2$ cells, as described below, and may represent the solid electrolyte interphase as postulated by the model. There were occasional cubic or needle-shaped crystals containing chloride scattered over the smooth salt layer. There were also crystals found on the glass surfaces.

We concluded that the crystalline lithium chloride observed in all these experiments formed partly by growth from species present in solution, and not solely in situ formation during corrosion at lithium surfaces. Solid lithium chloride could have been in equilibrium with dissolved LiCl, $LiAlCl_4$, or present in solution as the result of solvolysis reactions involving $B_{10}Cl_{10}^{2-}$, discussed below. The anion $B_{10}Cl_{10}^{2-}$ may serve to reduce the rate of LiCl crystal growth and resultant passivation by denying the lithium chloride a dissolved species with which it may rapidly exchange. The film which does exist on the lithium therefore cannot be attacked or altered by the electrolyte as easily. The solubility of LiCl itself is suppressed by the presence of the common ion, Li^+.

4.2 TASK II - PHYSICAL CHEMICAL PROPERTIES OF POLYHEDRAL BORATES IN $SOCl_2$

During measurements as a function of temperature for $SOCl_2/Li_2B_{10}Cl_{10}$, the conductivity was found to be dependent on the length of time after the solutions were prepared, increasing during a period of about one week. Subsequent analysis showed that lithium chloride was precipitating from the solutions as well, but that the polyhedral borate could be recovered quantitatively from the electrolyte by hydrolysis. Similar changes occurred in $SOCl_2/Li_2B_{12}Cl_{12}$, but much more slowly. Later investigation showed that the visible absorptivity of $Li_2B_{10}Cl_{10}/SOCl_2$ increased, and an electron paramagnetic resonance signal appeared and strengthened, during the same interval of time as the solvolysis and the increase in conductivity.

Steps should be taken to establish whether the presence of the radical bears any relationship to the effect which $Li_2B_{10}Cl_{10}$ has on the formation of the smooth chemically passivating layer on lithium stored in $SOCl_2$, and the alleviation of the voltage delay. Other salts or materials which are capable of forming free radicals in solutions of $LiAlCl_4/SOCl_2$ would be useful for this purpose.

The thermal stability of $Li_2B_{10}Cl_{10}$ and $Li_2B_{12}Cl_{12}$ was unexpectedly found to be limited. Following crystallization, these salts should be warmed under vacuum to remove water and ether present as solvates, but they cannot be warmed substantially above 200°C. The lower temperature, while requiring more time to remove the solvents, is necessary to prevent decomposition.

4.3 TASK III - ELECTROCHEMICAL PERFORMANCE OF Li/$SOCl_2$/C CELLS CONTAINING $Li_2B_{10}Cl_{10}$ OR $Li_2B_{12}Cl_{12}$ WHEN COMPARED WITH $LiAlCl_4$

We have confirmed that by using $Li_2B_{10}Cl_{10}$ as the electrolyte salt in lithium/thionyl chloride cells, the voltage delay on startup of cells after storage is substantially reduced when compared with cells containing $LiAlCl_4$, even if the storage and startup conditions are severe. While cells normally experienced a lower initial potential, none of the cells containing $Li_2B_{10}Cl_{10}/SOCl_2$ displayed a voltage delay deep enough or long enough to present a significant disadvantage when compared with fresh cells. Capacity and voltage delay tests with cells containing $Li_2B_{12}Cl_{12}$ were not conclusive, although the results indicated that the cells did not perform satisfactorily.

When $Li_2B_{10}Cl_{10}/SOCl_2$ was the electrolyte salt in $Li/SOCl_2$ cells, anode limited cells lost less capacity on storage than did similar cells with $LiAlCl_4/SOCl_2$. Our results indicate that the most important cause of anode corrosion in cells was through self-discharge by local cell reactions against electrically connected cell hardware. Previous work supports this conclusion (3). While lithium samples stored with electrolyte in glass ampoules without contacting cell hardware corroded less in $Li_2B_{10}Cl_{10}/SOCl_2$ than in $LiAlCl_4/SOCl_2$, the reduction in self-discharge against cell hardware in $Li_2B_{10}Cl_{10}/SOCl_2$ relative to $LiAlCl_4/SOCl_2$ was greater than could be explained solely on differences in corrosion by direct chemical reaction. Our results indicated that $Li_2B_{10}Cl_{10}$ reduced lithium loss from local discharge against hardware.

We recommend other lithium salts with dinegative ions or negative ions that will not exhange with solid LiCl for future study of the voltage delay problem. While the strong similarity in structure and chemistry between $Li_2B_{10}Cl_{10}$ and $Li_2B_{12}Cl_{12}$ would indicate parallel or similar behavior in $Li/SOCl_2$ cells, a real difference between cells employing these electrolytes would be significant in helping to determine whether the rate or extent of solvolysis affects the growth of the anode film. Other polyhedral borate salts such as $Li_2B_{10}Br_{10}$ might offer a means to compare the effects of the extent or rate of solvolysis, of the anion size or of free radical formation.

5. REFERENCES

1. A. N. Dey and C. R. Schlaikjer, Proc. Power Sources Symp. 26, 47 (1974).
2. A. N. Dey, Report DELET-TR-74-0109-F (July 1978).
3. N. Marincic and A. Lombardi, ECOM 74-0108-F (April 1977).
4. D. R. Cogley and M. J. Turchan, ECOM-0030-1 (February 1974).
5. J. R. Driscoll, et al., ECOM 74-0030-11 (October 1976).
6. E. Peled and H. Straze, J. Electrochem. Soc. 124, 1030 (1977).
7. Y. Avigal and E. Peled, J. Electroanal. Chem. 76, 135 (1977).
8. E. Peled and H. Yamin, submitted for publication to Proc. Power Sources Symp. 28 (1978).
9. E. Peled, Abstract No. 4, Electrochem. Soc. Fall Meeting, Atlanta, GA (October 1977).
10. E. Peled, C. R. Schlaikjer and N. Marincic, Abstract No. 553, Electrochem. Soc. Spring Meeting, Seattle, WA (May 1978).
11. L. Friedman and W. P. Wetter, J. Chem. Soc. 36 (1967).
12. C. R. Schlaikjer, F. Goebel and N. Marincic, J. Electrochem. Soc. 126, 513 (1979).
13. M. F. Hawthorne and R. L. Pilling, Inorg. Syntheses 9, 16 (1967).
14. H. C. Miller and E. L. Muetterties, Inorg. Syntheses 10, 81 (1967).
15. J. J. Auborn and N. Marincic, Power Sources 5, D. H. Collins, Ed., Proc. 9th Internatl. Symp., Brighton, England (September 1974), p. 683, Academic Press, London (1975).
16. N. Marincic and A. Lombardi, U.S. Patent No. 4,087,594.
17. N. Marincic, A. Lombardi and C. R. Schlaikjer, Proc. Power Sources Symp. 27, 37 (1976).
18. F. W. Dampier and P. E. Krouse, Abstract No. 23, Electrochem. Soc. Fall Meeting (October 1974).
19. J. D. Doe, F. W. Dampier, K. Jeffries, P. E. Krouse, N. Margalit, E. J. Merric, L. C. Thompson, Jr., Final Report AFAPL-TR-74-63, Contract No. F33615-72-C1470, ESB Inc. (December 1974).
20. C. R. Schlaikjer, U.S. Patent No. 4,020,240.
21. E. Peled and H. Yamin, submitted to the Israel J. of Chem.
22. C. R. Schlaikjer, submitted to 28th Power Sources Symp. (June 1978).
23. C. R. Schlaikjer, unpublished results.
24. A. N. Dey and J. Miller, J. Electrochem. Soc. 126, 1445 (1979).

25. A. N. Dey, U.S. Patent No. 4,071,664.

26. W. H. Knoth, H. C. Miller, J. C. Sauer, J. H. Balthis, Y. T. Chia and E. L. Meutterties, Inorg. Chem. 3, 159 (1964).

27. J. A. Forstner, T. E. Haas and E. L. Meutterties, Inorg. Chem. 3, 155 (1964).

28. E. L. Meutterties, J. Amer. Chem. Soc. 79, 6563 (1957).

29. F. A. Cotton and G. Wilkinson, Advanced Inorganic Chemistry, 3rd Ed., Wiley-Interscience, New York, p. 236 (1972).

30. R. D. Dobrot and W. N. Lipscomb, J. Chem. Phys. 37, 1779 (1962).

31. J. A. Wunderlick and W. N. Lipscomb, J. Amer. Chem. Soc. 82, 4427 (1960).

32. F. A. Cotton and G. Wilkinson, Advanced Inorganic Chemistry, 3rd Ed., Wiley-Interscience, New York, pp. 117-120 (1972).

33. J. S. Lewis and A. Kaczmarczyk, J. Amer. Chem. Soc. 88, 1068 (1966).

34. A. Kaczmarczyk, R. D. Dobrott and W. N. Lipscomb, Proc. Natl. Acad. Sci. U.S. 48, 729 (1962).

35. Z. B. Curtis, C. Young, R. Dickerson, K. K. Lai and A. Kaczmarczyk, Inorg. Chem. 13, 1760 (1974) and referenced literature.

36. R. L. Middaugh and F. Farha, Jr., J. Amer. Chem. Soc. 88, 4147 (1966).

37. W. H. Knoth, J. C. Sauer, D. C. England, W. R. Hertler and E. L. Muetterties, J. Amer. Chem. Soc. 86, 3973 (1964).

38. D. L. Chua, W. C. Merz and W. S. Bishop, "Proc. 26th Power Sources Symp., 33 (1976).

39. C. R. Schlaikjer, F. Goebel and N. Marincic, Abstract No. 16, Electrochem. Soc. Fall Meeting, Atlanta, GA (October 1977); J. Electrochem. Soc. 126, 513 (1979).

40. C. A. Young, M. S. Dobrusin and C. R. Schlaikjer, Report DELET-TR-0558-3 (November 1979).

41. J. M. West, "Electrodeposition and Corrosion Processes," D. van Nostrad, Princeton, NJ, pp. 100-123 (1965).

DISTRIBUTION LIST

101 Defense Technical Information Center
ATTN: DTIC-TCA
Cameron Station (Bldg. 5)
012 Alexandria, VA 22314

203 GIDEP Engineering & Support Dept.
TE Section
P.O. Box 398
001 NORCO, CA 91760

205 Director
Naval Research Laboratory
ATTN: CODE 2627
001 Washington, DC 20375

301 Rome Air Development Center
ATTN: Documents Library (TILD)
001 Griffiss AFB, NY 13441

437 Deputy for Science & Technology
Office, Asst. Sec. Army (R&D)
001 Washington, DC 20310

438 HQDA (DAMA-ARZ-D/Dr. F. D. Verderame)
001 Washington, DC 20310

482 Director
US Army Materiel Systems Analysis Actv
ATTN: DRXSY-MP
001 Aberdeen Proving Ground, MD 21005

563 Commander, DARCOM
ATTN: DRCDE
5001 Eisenhower Avenue
001 Alexandria, VA 22333

564 Cdr., US Army Signals Warfare Lab
ATTN: DELSW-OS
Vint Hill Farms Station
001 Warrenton, VA 22186

579 Cdr., PM Concept Analysis Centers
ATTN: DRCPM-CAC
Arlington Hall Station
001 Arlington, VA 22212

602 Cdr., Night Vision & Electro-Optics
ERADCOM
ATTN: DELNV-D
001 Fort Belvoir, VA 22060

603 Cdr., Atmospheric Sciences Lab
ERADCOM
ATTN: DELAS-SY-S
001 White Sands Missile Range, NM 88002

607 Cdr., Harry Diamond Laboratories
ATTN: DELHD-CO, TD (In Turn)
2800 Powder Mill Road
001 Adelphi, MD 20783

609 Cdr., ERADCOM
ATTN: DRDEL-CG, CD, CS (In Turn)
2800 Powder Mill Road
001 Adelphi, MD 20783

612 Cdr., ERADCOM
ATTN: DRDEL-CT
2800 Powder Mill Road
001 Adelphi, MD 20783

680 Commander
US Army Electronics R&D Command
000 Fort Monmouth, NJ 07703
    1 DELET-P
    1 DELEW-D
    1 DELET-DD
    1 DELSD-L (Tech Library)
    2 DELSD-L-S (STINFO)
    Originating Office
    (6) DELET-PR (W. Behl)

681 Commander
US Army Communications R&D Command
ATTN: USMC-LNO
001 Fort Monmouth, NJ 07703

705 Advisory Group on Electron Devices
201 Varick Street, 9th Floor
002 New York, NY 10014

DISTRIBUTION LIST (Continued)

Electrochimica
2485 Charleston Road
Mountain View, CA 94040
ATTN: Dr. Eisenberg (1)

Energy Storage & Conversion Dept.
TRW Systems
One Space Park
Redondo Beach, CA 90278 (1)

Power Conversion, Inc.
70 MaQuesten Parkway
Mount Vernon, NY 10550
ATTN: Stuart Chodosh (1)

Dr. D. Pouli
Portfolio Manager
Hooker Chemicals & Plastics Corp.
M.P.O. Box 8
Niagara Falls, NY 14302 (1)

Dr. Leonard Nanis
G207
S.R.I.
Menlo Park, CA 94025 (1)

Dr. J. J. Auborn, Rm. 1A-317
Bell Laboratories
600 Mountain Avenue
Murray Hill, NJ 07974 (1)

Stonehart Associates, Inc.
34 Five Fields Road
Madison, CT 06443
ATTN: Mr. Thomas Reddy (1)

Jet Propulsion Laboratory
4800 Oak Grove Drive
Pasadena, CA 91103
ATTN: Mr. Harvey Frank
Mail Stop 198-220 (1)

Dr. D. Ernst
Naval Surface Weapons Center
White Oak Laboratory, Code R-33 (M/S A026)
Silver Spring, MD 20910 (1)

Mr. J. R. Moden
Energy Conversion Branch Code 3642
Naval Underwater Systems Center
Newport Laboratory
Newport, RI 02840 (1)

NASA Lewis Research Center
Mail Stop 6-1
21000 Brookpark Road
Cleveland, OH 44135
ATTN: Dr. Stuart Fordyce (1)

Mr. Joe McCartney
Naval Undersea Center
Code 608
San Diego, CA 92132 (1)

EIC, Inc.
ATTN: S. B. Brummer
Newton, MA 02158 (1)

Altus Corp.
440 Page Mill Road
Palo Alto, CA 94306
Attn: Douglas Glader (1)

J. Bene
MS 488
NASA Langley Research Center
Hampton, VA 23665 (1)

Mr. Eddie T. Seo
Research and Development Div.
The Gates Rubber Co.
999 S. Broadway
Denver, CO 80217 (1)

Mr. Sidney Gross
Mail Stop 8C-62
Boeing Aerospace Company
P.O. Box 3999
Seattle, WA 98124 (1)

Honeywell Technology Center
ATTN: Dr. H. V. Venkatasetty
10701 Lyndale Avenue South
Bloomington, MN 55420 (1)

Mr. Aiji Uchiyama
Jet Propulsion Laboratory - M.S. 198-22
4800 Oak Grove Drive
Pasadena, CA 91103 (1)

Dr. Frank Bis
Naval Surface Weapons Center
White Oak Laboratory, Code R-33
Silver Spring, MD 20910 (1)

DISTRIBUTION LIST (Continued)

CMDR., MICOM
ATTN: DRCPM-HDE
Redstone Arsenal, AL 35809 (1)

Transportation Systems Center
Kendall Square
Cambridge, MA 02142
ATTN: Dr. Norman Rosenberg (1)

Foote Mineral Company
Route 100
Exton, PA 19341
ATTN: Dr. H. Grady (1)

Honeywell, Inc.
104 Rock Road
Horsham, PA 19044 (1)

Sanders Associates, Inc.
Sonobuoy Division
95 Canal Street
Nashua, NH 03060
ATTN: Mr. David Dwyer (1)

Eagle-Picher Industries, Inc.
Electronics Division
ATTN: Mr. Robert L. Higgins
P.O. Box 47
Joplin, MO 64801 (1)

Yardney Electric Company
82 Mechanic Street
Pawcatuck, CT 06379
ATTN: Technical Library (1)

P. R. Mallory & Co., Inc.
Northwest Industrial Park
Burlington, MA 01803
ATTN: Dr. A. N. Dey

Exxon Research & Engineering Co.
Corporate Research Laboratory
Linden, NJ 07036
ATTN: Dr. R. Hamlen (1)

Argonne National Laboratories
9700 South Cass
Argonne, IL 60439
ATTN: Dr. E. C. Gay (1)

GTE Sylvania Incorporated
77 A Street
Needham Heights, MA 02194
ATTN: Mr. Richard Pabst (1)

General Motors Corporation
Research Laboratories
General Motors Technical Center
12 Mile and Mounds Roads
Warren, MI 48090
ATTN: Dr. J. L. Hartman (1)

Union Carbide Corporation
Parma Research Center
P.O. Box 6116
Cleveland, OH 44101 (1)

P. R. Mallory & Co., Inc.
S. Broadway
Tarrytown, NY 10591
ATTN: J. Dalfonso (1)

North American Rockwell Corp.
Atomics International Division
Box 309
Canoga Park, CA 91304
ATTN: Dr. L. Heredy (1)

General Electric Research &
Development Center
P.O. Box 8
Schenectady, NY 12301
ATTN: Dr. Stefan Mitoff (1)

The Electric Storage Battery Co.
Carl F. Norbury Research Center
19 West College Avenue
Yardley, PA 19067
ATTN: Dr. A. Salkind (1)

Gulton Industries, Inc.
Metuchen, NJ 08840
ATTN: Mr. S. Charlip (1)

Reliability Analysis Center
Griffiss AFB, NY 13441 (1)

DATE
ILMED

-8